NOTE 349

A COUPLING MODEL FOR A PAIR OF SKEWED TRANSMISSION LINES

by

David V. Giri
Steve K. Chang
Fred M. Tesche

12 September 1978

A COUPLING MODEL FOR A PAIR OF SKEWED TRANSMISSION LINES

ABSTRACT

A coupling model in the form of an equivalent circuit is developed for a pair of skewed transmission lines. The inductive coupling is evaluated in closed form and the capacitances are obtained from the solution of a pair of coupled integral equations for the excess charge distributions along the transmission lines. The coupled integral equations for the excess charges are solved by an approximate analytical method and also by employing the method of moments. The two solutions are seen to be in excellent agreement. The excess charge distributions are then used in a parametric study of the capacitances in the coupling model. The results are presented in graphical form.

CONTENTS

I. Introduction and Problem Definition

This report addresses a rather specific problem in the area of multiconductor transmission theory. Specifically, we desire to obtain an equivalent circuit in the vicinity of the junction region of two skewed transmission lines, so that the coupling of energy from one line to another can be estimated. It is noted that the term "junction" does not refer to lines in physical contact, but rather the position of smallest separation between the lines. The geometry of the problem is shown in Figure 1.1. It consists of a two-wire transmission line of characteristic impedance Z_{c2} passing over another two-wire transmission line of characteristic impedance Z_{c1}. The wires 1 and 2 in Figure 1.1 are both parallel to a perfectly conducting ground plane and are located at heights of h_1 and h_2 respectively. The wires are assumed to be of the same radius, although this is not essential. Figure 1.2 shows an equivalent geometry with the image conductors; the relevant distances between source and observation points are also indicated. As illustrated in this figure, the two lines are modelled by closed rectangular loops by introducing the vertical segments at both ends.

The objective is to compute the elements of a coupling model in the form of an equivalent circuit. In general, for arbitrary values of θ in the range of $[0 < \theta \leq (\pi/2)]$, one would expect inductive and capacitive coupling between the transmission lines. The special case of $\theta = 0$ is precluded here because of the distributed nature of the coupling which cannot be treated with localized lumped elements. Appendix A includes

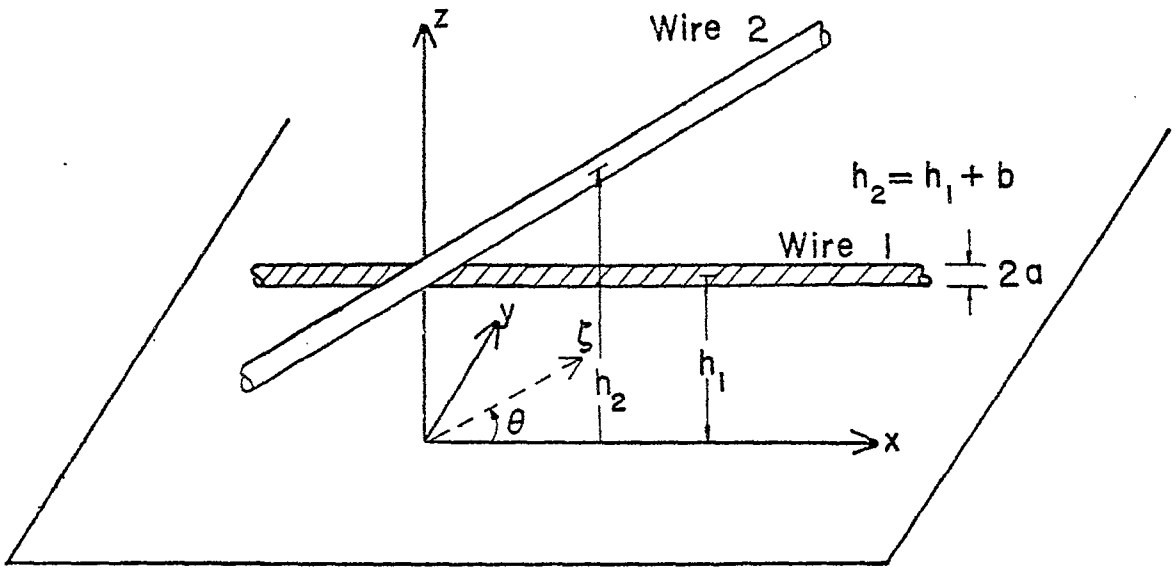

Figure 1.1. Two skewed wires of the same radius above an image plane.

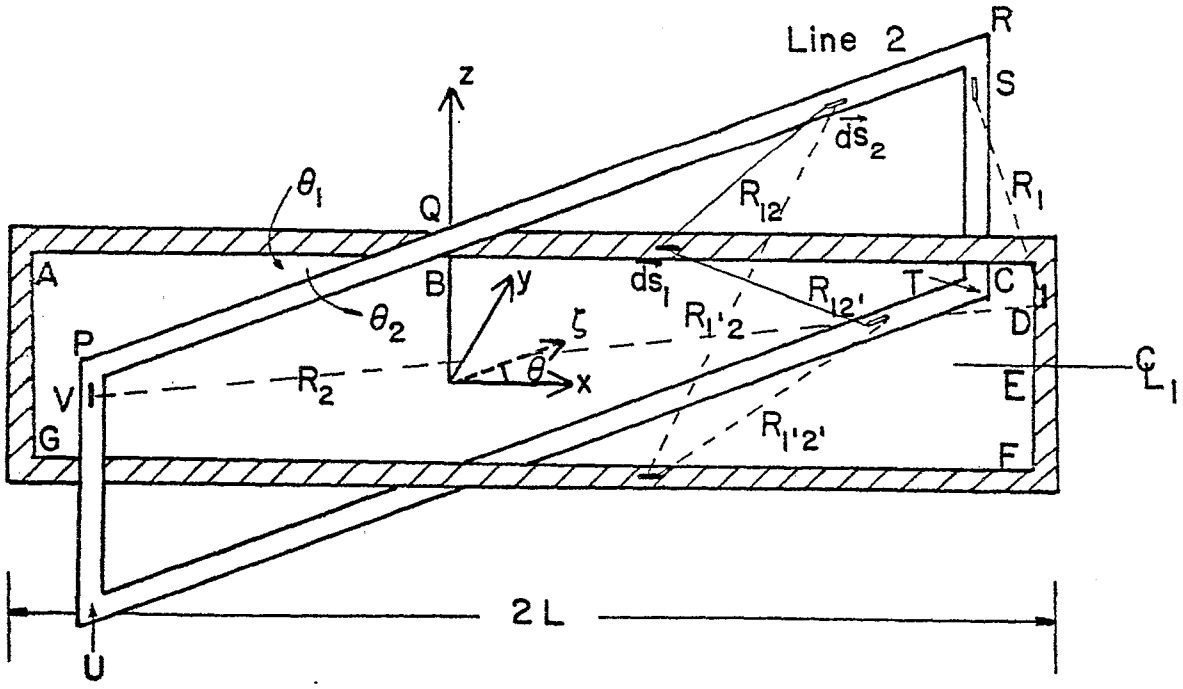

Figure 1.2. Equivalent pair of skewed two-wire transmission lines of length 2L.

this special case, reported elsewhere [1], for the sake of completeness.

For values of θ in the range of $[0 < \theta \leq (\pi/2)]$, the inductive-capactive coupling may be represented by a junction equivalent circuit of Figure 1.3. In this figure, C_{1j} and C_{2j} are the lumped capacitances in lines 1 and 2 owing to the junction. That is, C_{1j} is computed from the excess line capacitance of line 1, due to the presence of line 2, for a distance of sufficient magnitude away from the junction on both sides. C_{mj} is the lumped mutual capacitance. The inductive coupling is shown in the form of a transformer comprised of self inductances L_{1j} and L_{2j}, as well as a mutual inductance L_{mj}. To display the symmetry, the inductive circuit should be denoted with half of the nominal values on either side of the junction. However, we immediately recognize that since the wires are assumed to be electrically thin and perfect conductors, there is negligible reduction in the self-inductance of each wire, due to the proximity of the other wire. This implies that $L_{1j} = L_{2j} = 0$ and results in only inductive coupling via L_{mj}. Figure 1.4 shows the coupling model after setting the excess self-inductances to zero and representing the mutual inductances by appropriate voltage sources. Figure 1.5a is essentially the same as Figure 1.4, showing the equivalent circuit model above the image plane. In Figure 1.5b, we show the symmetric form of the coupling model and the potentials on all the four lines with respect to the image plane which is chosen as the reference potential.

Note:
The inductive circuit is shown on one side of the junction for convenience only.

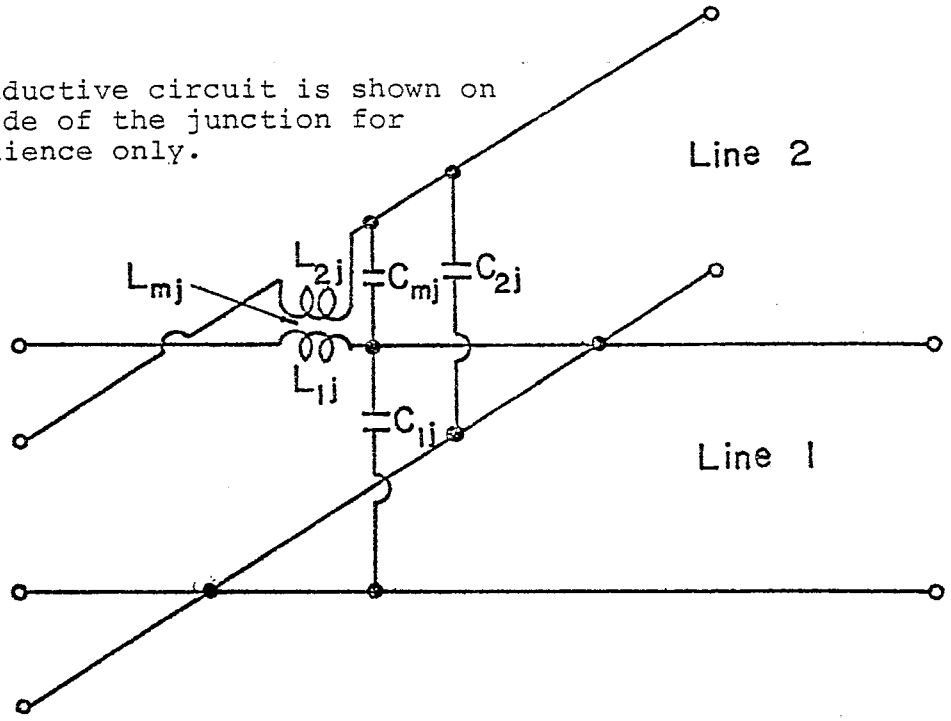

Figure 1.3. A generalized coupling model for the junction of two skewed transmission lines.

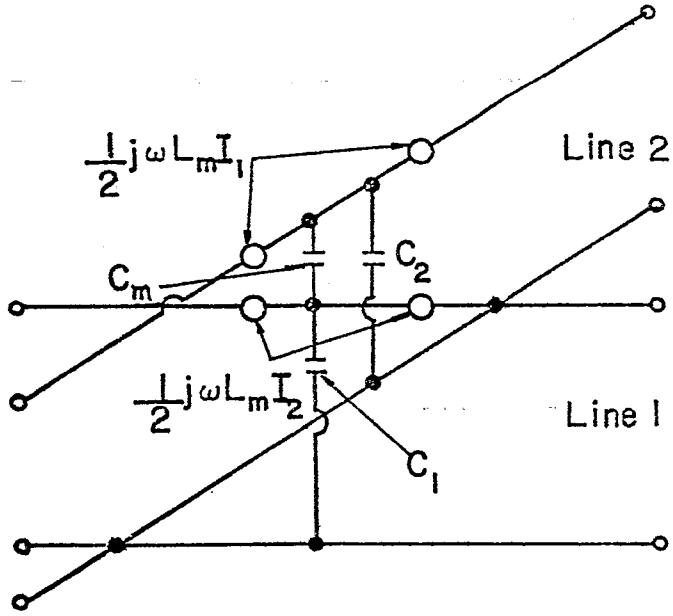

Figure 1.4. Coupling model showing the mutual inductance as voltage sources; (note that the subscript j, denoting the junction has been dropped).

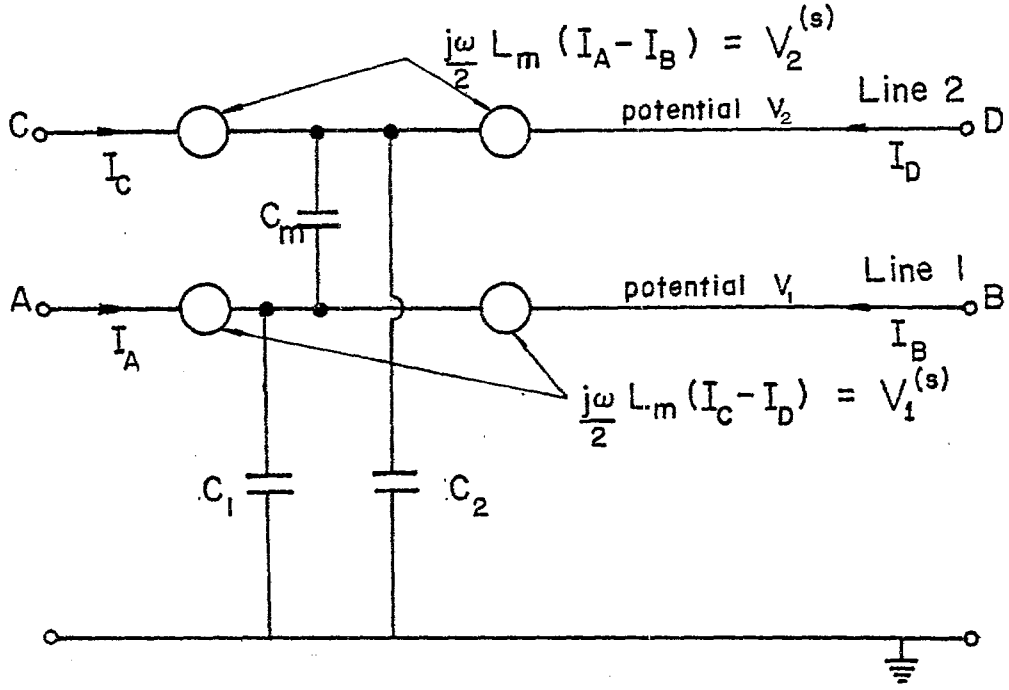

Figure 1.5a. Equivalent circuit above the image plane.

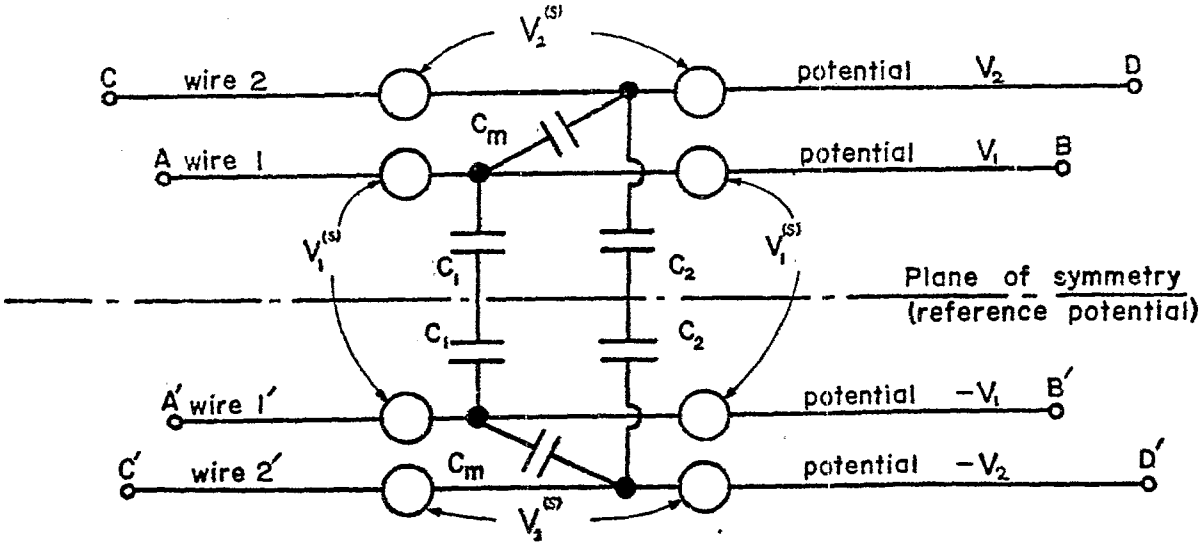

Figure 1.5b. Symmetrical form of the above circuit.

The problem at hand then, is to determine the elements L_m, C_1, C_2 and C_m. For ease of data presentation, we define a set of normalized lumped parameters as follows.

$$\begin{aligned} L_m^{(n1)} &= L_m/(h_1 L'_1) \\ C_1^{(n1)} &= C_1/(h_1 C'_1) \\ C_2^{(n2)} &= C_2/(h_2 C'_2) \\ C_m^{(n1)} &= C_m/(h_1 C'_1) \end{aligned} \tag{1.1}$$

The superscript n1 in the above equation indicates normalization with respect to the line constants of line 1 and likewise for n2. Some preliminary information concerning the two isolated transmission lines is given below in Table 1. Note that the image plane is chosen as the reference potential.

TABLE I. PRELIMINARY INFORMATION ABOUT THE TWO ISOLATED TRANSMISSION LINES.

Parameter	Line 1	Line 2
radius	$a \quad (a \ll h_1)$	$a \quad (a \ll h_2)$
separation	$2h_1$	$2h_2$
inductance/ unit length	L'_1 $\simeq \frac{\mu_o}{2\pi} \ln(2h_1/a)$	L'_2 $\simeq \frac{\mu_o}{2\pi} \ln(2h_2/a)$
capacitance/unit length	C'_1 $\simeq 2\pi\varepsilon_o/\ln(2h_1/a)$	C'_2 $\simeq 2\pi\varepsilon_o/\ln(2h_2/a)$
characteristic impedance	$\sqrt{L'_1/C'_1}$ $\simeq 60 \ln(2h_1/a)$	$\sqrt{L'_2/C'_2}$ $\simeq 60 \ln(2h_2/a)$

II. Mutual Inductance

In this section, we evaluate the mutual inductance element L_m between the two skewed transmission lines of Figure 1.2. It is believed that more insight into the problem is gained by looking at the skewed transmission lines of finite length $2L$ and later let L tend to infinity. The assumptions made in the following analysis are listed below.

$$L >> h_> \qquad \text{(long lines)} \tag{2.1a}$$

$$(h_> - h_<) >> a \qquad \text{(sufficiently apart)} \tag{2.1b}$$

$$0 < \theta < (\pi/2), \text{ but } \theta \neq 0 \text{ (no distributed interaction)} \tag{2.1c}$$

$$(\partial/\partial\theta_1)(\text{charge distribution}) \equiv 0 \quad \text{(thin wire approximation}$$
$$(\partial/\partial\theta_2)(\text{charge distribution}) \equiv 0 \quad \text{or rotational symmetry)} \tag{2.1d}$$

where $h_<$ and $h_>$ are respectively smaller and larger of h_1 and h_2. With the above assumptions, one can write the mutual inductance as [2],

$$L_m \simeq \left[\frac{\mu_o}{4\pi} \oint_{C_1} \vec{ds}_1 \cdot \oint_{C_2} \frac{1}{R_{12}} \vec{ds}_2 \right] \tag{2.2}$$

where

μ_o = free space permeability = $4\pi \times 10^{-7}$ (H/m), and C_1 and C_2 represent the closed (assumed) loops formed by the two transmission lines. With reference to Figure 1.2, we can formally write

$$L_m \simeq \frac{\mu_o}{4\pi} \oint_{\substack{ABCD \\ EFGA}} \vec{ds}_1 \cdot \oint_{\substack{PQRS \\ TUVP}} \vec{ds}_2 \left(\frac{1}{R}\right)$$

Taking advantage of symmetry, we have

$$L_m \simeq \frac{\mu_o}{\pi} \int_{BCDE} \vec{ds}_1 \cdot \int_{\substack{PQRS \\ TUVP}} \vec{ds}_2 \left(\frac{1}{R}\right) \tag{2.3}$$

Since there is no inductive interaction between the sections of transmission lines that are orthogonal, equation (2.3) simplifies to

$$L_m \simeq \frac{\mu_o}{\pi} \left[\cos(\theta) \int_0^L dx \int_{-L}^{L} \left(\frac{1}{R_{12}} - \frac{1}{R_{12'}}\right) d\xi + \int_0^{h_1} dz_1 \int_{-h_2}^{h_2} \left(\frac{1}{R_1} - \frac{1}{R_2}\right) dz_2 \right] \tag{2.4a}$$

$$= \frac{\mu_o}{\pi} [\cos(\theta) I_1(\theta) + I_2(\theta)] \tag{2.4b}$$

In view of the assumptions of equation (2.1), the R's in the above equation may be approximated by

$$R_{12} \simeq [x^2 + \xi^2 - 2x\xi \cos(\theta) + (h_2 - h_1)^2]^{\frac{1}{2}} \tag{2.5a}$$

$$R_{12'} \simeq [x^2 + \xi^2 - 2x\xi \cos(\theta) + (h_2 + h_1)]^{\frac{1}{2}} \tag{2.5b}$$

$$R_1 \simeq [(z_2 - z_1)^2 + 4L^2 \sin^2(\theta/2)]^{\frac{1}{2}} \tag{2.5c}$$

$$R_2 \simeq [(z_2 - z_1)^2 + 4L^2 \cos^2(\theta/2)]^{\frac{1}{2}} \tag{2.5d}$$

We will now proceed to evaluate the two integrals $I_1(\theta)$ and $I_2(\theta)$ separately. Setting

$$\alpha = |(h_2 - h_1)| \quad \text{and} \quad \beta = (h_2 + h_1) \tag{2.6}$$

$I_1(\theta)$ is given by

$$I_1(\theta) = \int_0^L dx \int_{-L}^{L} \left(\frac{1}{\sqrt{x^2+\xi^2-2x\xi \cos(\theta)+\alpha^2}} - \frac{1}{\sqrt{x^2+\xi^2-2x\xi \cos(\theta)+\beta^2}} \right) d\xi$$

$$= \int_0^L dx \left[\int_0^L \left(\frac{1}{\sqrt{x^2+\xi^2-2x\xi \cos(\theta)+\alpha^2}} - \frac{1}{\sqrt{x^2+\xi^2-2x\xi \cos(\theta)+\beta^2}} \right) d\xi \right.$$

$$\left. + \int_0^L \left(\frac{1}{\sqrt{x^2+\xi^2+2x\xi \cos(\theta)+\alpha^2}} - \frac{1}{\sqrt{x^2+\xi^2+2x\xi \cos(\theta)+\beta^2}} \right) d\xi \right]$$

$$= \int_0^L dx \left[I_{11}(x,\theta) + I_{11}(x,\pi-\theta) \right] \tag{2.7}$$

where

$$I_{11}(x,\theta) = \int_0^L d\xi \left(\frac{1}{\sqrt{(x^2+\alpha^2)+[-2x \cos(\theta)]\xi+\xi^2}} - \frac{1}{\sqrt{(x^2+\beta^2)+[-2x \cos(\theta)]\xi+\xi^2}} \right) \tag{2.8}$$

This integral may be performed using the result 2.261 of reference [3],

$$I_{11}(x,\theta) = \ln\left\{\frac{\sqrt{x^2+\alpha^2-2xL\cos(\theta)+L^2}+L-[x\cos(\theta)]}{\sqrt{x^2+\beta^2-2xL\cos(\theta)+L^2}+L-[x\cos(\theta)]}\right\}$$

$$+\ln\left\{\frac{\sqrt{x^2+\beta^2}-x\cos(\theta)}{\sqrt{x^2+\alpha^2}-x\cos(\theta)}\right\} \qquad (2.9)$$

$$=\ln\left\{\frac{\sqrt{x^2+\beta^2}-x\cos(\theta)}{\sqrt{x^2+\alpha^2}-x\cos(\theta)}\right\}+ I_n(x,\theta)$$

where $I_n(\theta)$ is the first term on the right side of equation (2.9). Therefore,

$$I_{11}(x,\pi-\theta) = \ln\left\{\frac{\sqrt{x^2+\beta^2}+x\cos(\theta)}{\sqrt{x^2+\alpha^2}+x\cos(\theta)}\right\}+ I_n(x,\pi-\theta) \qquad (2.10)$$

Substituting the above two equations into equation (2.7), we obtain,

$$I_1(\theta) = \left[\int_0^L dx\ \ln\left\{\frac{x^2+\beta^2\ \mathrm{cosec}^2(\theta)}{x^2+\alpha^2\ \mathrm{cosec}^2(\theta)}\right\}\right]+\int_0^L I_n(x,\theta)\ dx$$

$$+\int_0^L I_n(x,\pi-\theta)\ dx \qquad (2.11)$$

Using the result 2.733.1 of reference [3],

$$I_1(\theta) = L\ \ln\left\{\frac{L^2+\beta^2\ \mathrm{cosec}^2(\theta)}{L^2+\alpha^2\ \mathrm{cosec}^2(\theta)}\right\} + \left[\frac{2\beta}{\sin(\theta)}\arctan\left|\frac{L\sin(\theta)}{\beta}\right|\right]$$

$$-\left[\frac{2\alpha}{\sin(\theta)}\arctan\left|\frac{L\sin(\theta)}{\alpha}\right|\right]$$

$$+\left[i_n(\theta)+i_n(\pi-\theta)\right] \qquad (2.12)$$

where $i_n(\theta)$ is an integral to be evaluated numerically and is given by

$$i_n(\theta) = \int_0^L I_n(x,\theta)\, dx$$

$$= \int_0^L \ell n \left\{ \frac{\sqrt{x^2+\alpha^2-2xL\cos(\theta)+L^2}+L-[x\cos(\theta)]}{\sqrt{x^2+\beta^2-2xL\cos(\theta)+L^2}+L-[x\cos(\theta)]} \right\} dx \qquad (2.13)$$

It may be shown that, when the lengths of the transmission lines are large compared to the heights, $i_n(\theta)$ does not contribute significantly to the result in equation (2.12). We still have the second term of equation (2.4a) to compute, which accounts for the interaction between the vertical end wires and it is given by

$$I_2(\theta) = \int_0^{h_1} dz_1 \int_{-h_2}^{h_2} dz_2 \left(\frac{1}{\sqrt{(z_2-z_1)^2 + A_1^2}} - \frac{1}{\sqrt{(z_2-z_1)^2 + A_2^2}} \right) \qquad (2.14a)$$

where

$$A_1 = 2L \sin(\theta/2); \quad A_2 = 2L\cos(\theta/2) \qquad (2.14b)$$

Consider the first term on the right side of the above,

$$\text{Integral} = \int_0^{h_1} dz_1 \int_{-h_2}^{h_2} dz_2 \left(\frac{1}{\sqrt{(z_2-z_1)^2 + A_1^2}} \right) \qquad (2.15)$$

Using (2.261.2 of Ref. [3]), we can evaluate this integral to be

$$= \int_0^{h_1} dz_1 \left[\text{arcsinh} \left\{ \frac{h_2 - z_1}{A_1} \right\} + \text{arcsinh} \left\{ \frac{h_2 + z_1}{A_1} \right\} \right]$$

$$= A_1 \left[\int_{(h_2/A_1)}^{(\beta/A_1)} \text{arcsinh}\ (y)\ dy - \int_{(h_2/A_1)}^{(\alpha/A_1)} \text{arcsinh}\ (y)\ dy \right]$$

$$= A_1 \left[\int_{(\alpha/A_1)}^{(\beta/A_1)} \text{arcsinh}\ (y)\ dy \right]$$

using (2.741.2. of [3]), we get

$$= \left[\beta\ \text{arcsinh}\ (\beta/A_1) - \alpha\ \text{arcsinh}\ (\alpha/A_1) - \sqrt{\beta^2 + A_1^2} + \sqrt{\alpha^2 + A_1^2} \right] \tag{2.16}$$

Therefore

$$\begin{aligned} I_2(\theta) = {} & \beta \left[\text{arcsinh}\ (\beta/A_1) - \text{arcsinh}\ (\beta/A_2) \right] \\ & - \alpha \left[\text{arcsinh}\ (\alpha/A_1) - \text{arcsinh}\ (\alpha/A_2) \right] \\ & - \left[\sqrt{\beta^2 + A_1^2} - \sqrt{\beta^2 + A_2^2} \right] \\ & + \left[\sqrt{\alpha^2 + A_1^2} - \sqrt{\alpha^2 + A_2^2} \right] \end{aligned} \tag{2.17}$$

Substituting our results for $I_1(\theta)$ and $I_2(\theta)$ from equations (2.12) and (2.17) respectively into equation (2.4b), we finally obtain for the mutual inductance

$$L_m \simeq \frac{\mu_o}{\pi}\Bigg[L \ln\left\{\frac{1 + \frac{\beta^2}{L^2}\csc^2(\theta)}{1 + \frac{\alpha^2}{L^2}\csc^2(\theta)}\right\}\cos(\theta) + \left\{i_n(\theta) + i_n(\pi-\theta)\right\}\cos(\theta)$$

$$+ \left\{\frac{2\beta}{\sin(\theta)}\arctan\left(\frac{L\sin\theta}{\beta}\right) - \frac{2\alpha}{\sin(\theta)}\arctan\left(\frac{L\sin\theta}{\alpha}\right)\right\}\cos(\theta)$$

$$+ \beta\left\{\text{arcsinh}(\beta/A_1) - \text{arcsinh}(\beta/A_2)\right\}$$

$$- \alpha\left\{\text{arcsinh}(\alpha/A_1) - \text{arcsinh}(\alpha/A_2)\right\}$$

$$- \left\{\sqrt{\beta^2 + A_1^2} - \sqrt{\beta^2 + A_2^2}\right\}$$

$$+ \left\{\sqrt{\alpha^2 + A_1^2} - \sqrt{\alpha^2 + A_2^2}\right\}\Bigg] \qquad (2.18)$$

We recall that in the above expression, the various quantities are

L = half length of the transmission lines

θ = skew angle

$\beta = (h_1 + h_2)$; $\alpha = |h_2 - h_1|$

$A_1 = 2L \sin(\theta/2)$; $A_2 = 2L \cos(\theta/2)$

μ_o = free space permeability

and $i_n(\theta)$, given in equation (2.13), is an integral which can be evaluated numerically, however small its contribution may be.

A. Discussion of Results

Equation (2.18) is the mutual inductance of two skewed transmission lines each of length 2L. It is interesting to note that for finite values of heights h_1 and h_2 and the skew angle in the range of $0 < \theta < (\pi/2)$, and letting the length of the transmission lines tend to infinity, the mutual inductance becomes

$$\lim_{L \to \infty} \quad L_m = \mu_o(\beta-\alpha) \cot(\theta)$$
$$= \mu_o[(h_2+h_1) - |h_2-h_1|] \cot(\theta)$$
$$= 2\mu_o h_< \cot(\theta) \qquad (2.19)$$

with $h_<$ being the smaller of (h_1 and h_2).

This result has been independently verified by starting the problem with infinitely long lines. It suggests that if the transmission lines are infinitely long, the mutual inductance is a property of only the transmission line with smaller spacing.

However, under the assumptions outlined in equation (2.1), equation (2.18) accurately gives the value of the mutual inductance and is parametrically displayed in Figures 2.1, 2.2, and 2.3. The quantity plotted is the normalized mutual inductance $L_m^{(nl)}$ of equation (1.1) given by

$$L_m^{(nl)} = L_m \Big/ \left[h_1 L_1'\right] \qquad \text{(dimensionless)}$$

$$= L_m \Big/ \left[h_1 \left(\frac{\mu_o}{2\pi}\right) \ell n \left(\frac{2h_1}{a}\right)\right] \qquad (2.20)$$

All linear dimensions are normalized with respect to h_1 by choosing $h_1 = 1$. The radius a is chosen to be .01347 so that $\ell n(2h_1/a) = 5$ and it occurs only in the normalization procedure. With this choice of normalization, $L_m^{(nl)}$ is a function of three variables, θ, h_2 and L. In Figures 2.1, 2.2, and 2.3, $L_m^{(nl)}$ is shown plotted as a function of these three variables respectively. In computing $L_m^{(nl)}$ from equation (2.20), the "exact" expression of L_m given by equation (2.18) is used which includes the contribution from the end wires as well. The two integrals appearing in equation (2.18) have smooth integrands and a simple Simpson's rule of integration was found to be adequate.

As a function of the skew angle θ, the mutual inductance in Figure 2.1 goes to zero at $\theta = (\pi/2)$, as one would expect. In this figure, one can see the insensitivity of the mutual inductance with respect to h_2 even for small θ as the lengths of the transmission line increase. For all the four cases of varying L, it is seen that for $\theta = 0$, the mutual inductance displays a singularity corresponding to the transmission line or distributed type of interaction.

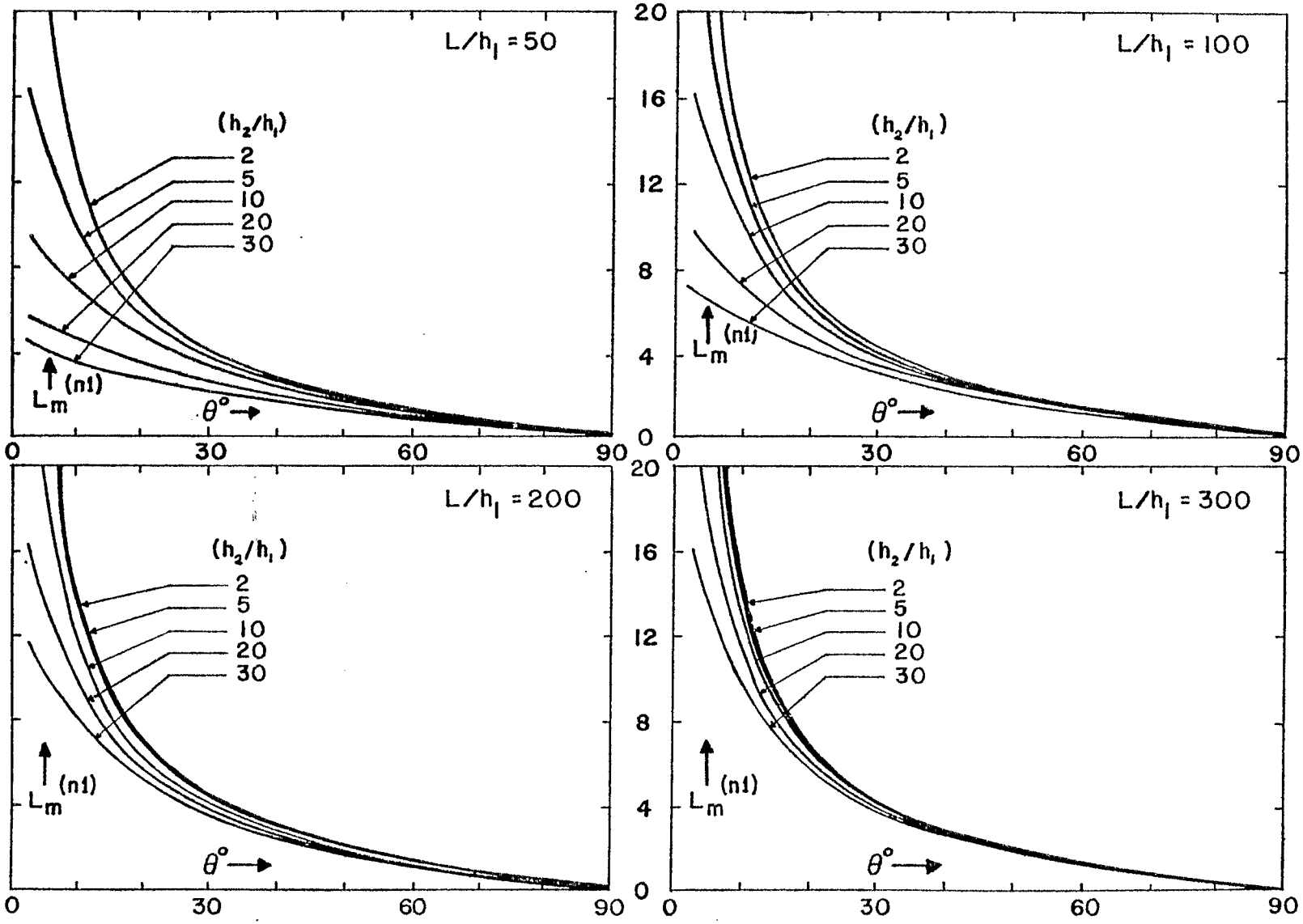

Figure 2.1 Normalized mutual inductance as a function of the skew angle θ

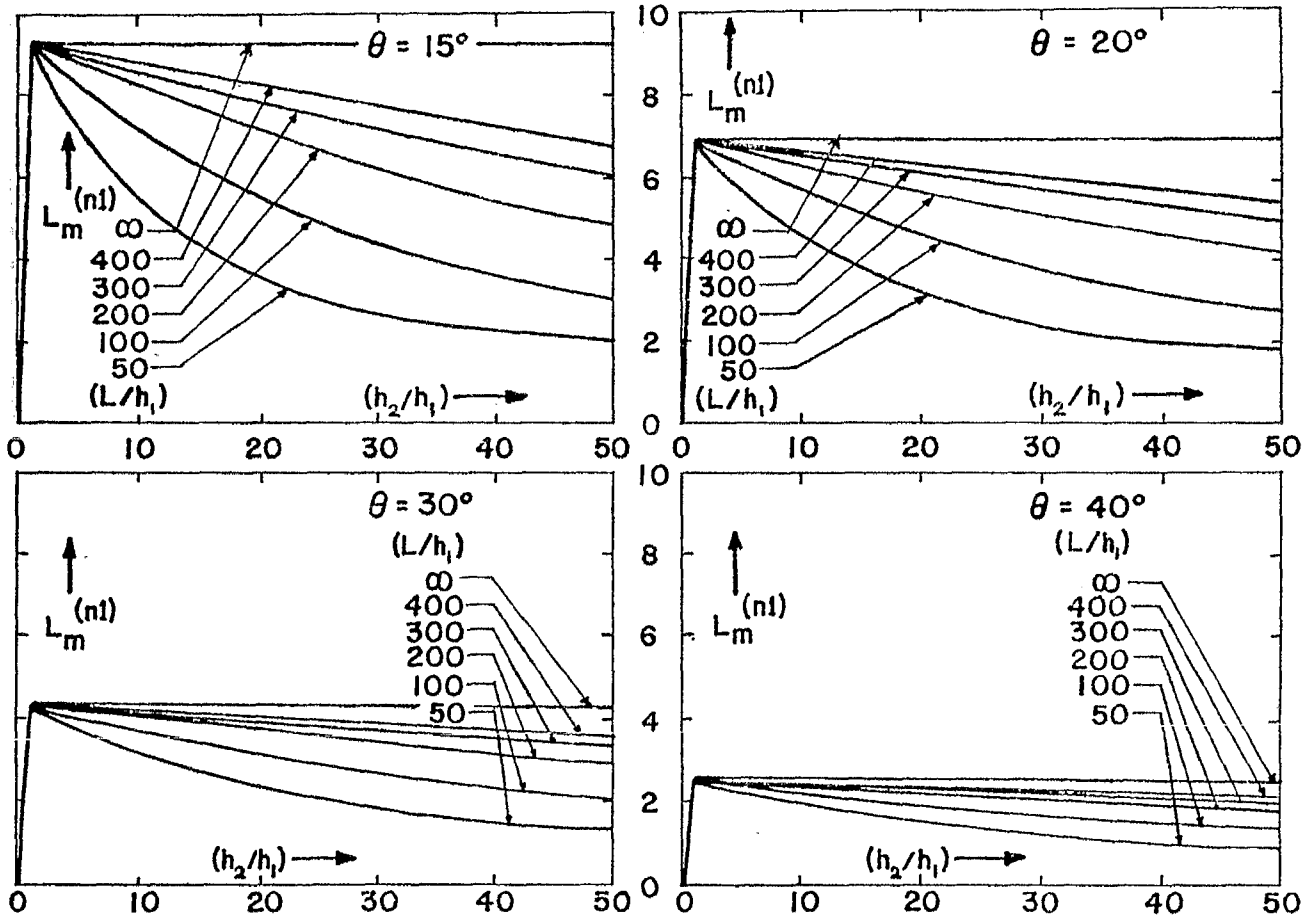

Figure 2.2 Normalized mutual inductance as a function of the relative height (h_2/h_1).

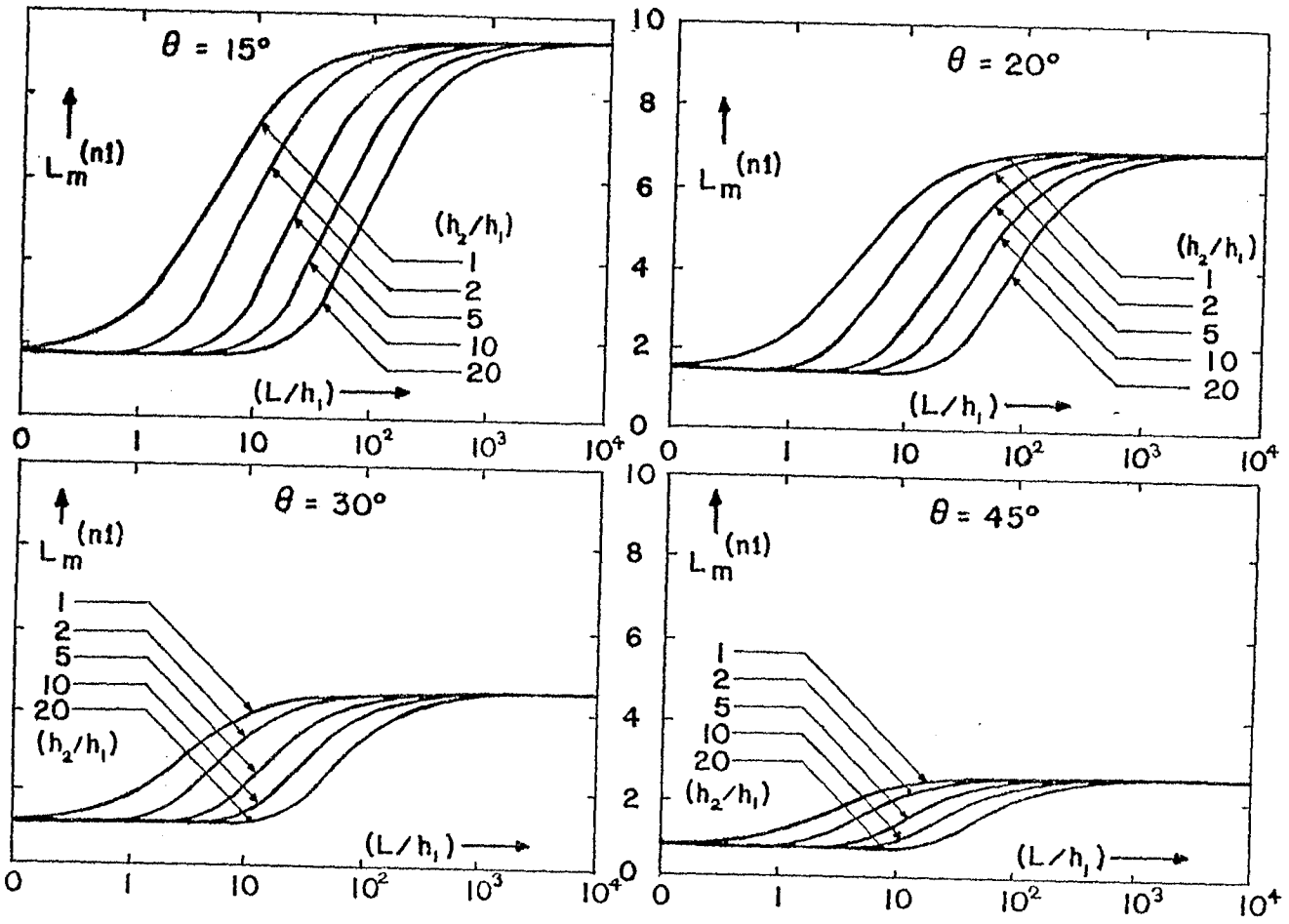

Figure 2.3 Normalized mutual inductance as a function of normalized line length (L/h_1).

In Figure 2.2, the normalized mutual inductance is plotted as a function of (h_2/h_1), for a fixed skew angle θ and with the length (L/h_1) as a parameter. The four values of θ considered are = 15°, 20°, 30°, 45°. For all these cases, the normalized mutual inductance is zero initially $[(h_2/h_1) = 0]$ and reaches a peak when $[(h_2/h_1) = 1]$ and monotonically decreases as (h_2/h_1) is increased beyond the value of unity. Also, as one would expect, the peak value itself is decreasing as θ is increased and the normalized mutual inductance tends to zero for the orthogonal case of $\theta = 90°$.

Finally in Figure 2.3, the normalized mutual inductance is shown plotted as a function of the length of the wires (L/h_1) with the relative height (h_2/h_1) as a parameter. Note that the normalized length (L/h_1) is plotted on a logarithmic scale and the same four values of θ as before are considered. These plots show that at the two extreme values $[(L/h_1) \to 0$ and $(L/h_1) >> 1]$, the normalized mutual inductance tends to values that are independent of (h_2/h_1). The residual value when $(L/h_1) = 0$ accounts for the interaction between the vertical end members of the transmission lines. However, for large lengths $L >> h_>$, the mutual inductance is seen to obtain a value which is dependent only on $h_<$ (see equation 2.19). We reach an interesting conclusion that, if the

transmission lines are infinitely long, the mutual inductance is a property of only the transmission line with the smaller wire separation.

III. Capacitive Coupling

The physical mechanism that justifies the use of a capacitive coupling model of Figure 1.5 may be described as follows. When the two lines are present by themselves and unperturbed by the other, the total charge per unit length on the two wires are constants given by Q'_{10} and Q'_{20} ([4]). The effect of the proximity of one wire on the other results in a redistribution of charge in the vicinity of the junction so that the total charges per unit lengths $Q'_1(x,\theta)$ and $Q'_2(\zeta,\theta)$ now become position dependent according as

$$Q'_1(x,\theta) = Q'_{10} + q'_1(x,\theta)$$

$$Q'_2(\zeta,\theta) = Q'_{20} + q'_2(\zeta,\theta) \qquad (3.1)$$

where the excess total charges per unit length $q'_1(x,\theta)$ and $q'_2(\zeta,\theta)$ permit us to derive a capacitive coupling model. Implicit in such a derivation is an assumption [4] that the excess charges which decay with distance away from the junction will have an integrated effect and can be represented by lumped parameters at the junction itself.

We also note here that for the case of $\theta = 0$, the total charges per unit length once again become independent of position, denoted by

$$Q'_1(x,0) \equiv Q'_{10} = (Q'_{10} + q'_{10})$$
$$Q'_2(\zeta,0) \equiv Q'_{20} = (Q'_{20} + q'_{20}) \tag{3.2}$$

where the excess charges for the case of $\theta = 0$ also are constants according as

$$q'_1(x,0) \equiv q'_{10}$$
$$q'_2(\zeta,0) \equiv q'_{20} \tag{3.3}$$

The entire electrostatic system for all values of θ is electrically neutral because the image wires carry exact amounts of opposite charges, i.e.,

$$\left[Q'_{1'}(x,\theta) = -Q'_1(x,\theta)\right] \quad ; \quad \left[Q'_{2'}(\zeta,\theta) = -Q'_2(\zeta,\theta)\right]$$
$$\left[q'_{1'}(x,\theta) = -q'_1(x,\theta)\right] \quad ; \quad \left[q'_{2'}(\zeta,\theta) = -q'_2(\zeta,\theta)\right] \tag{3.4}$$

Furthermore, by virtue of symmetry about the junction, all the charges are even functions in their respective variables, as shown below.

$$\left[Q'_1(x,\theta) = Q'_1(-x,\theta)\right] \quad ; \quad \left[Q'_2(\zeta,\theta) = Q'_2(-\zeta,\theta)\right]$$
$$\left[q'_1(x,\theta) = q'_1(-x,\theta)\right] \quad ; \quad \left[q'_2(\zeta,\theta) = q'_2(-\zeta,\theta)\right] \tag{3.5}$$

For θ in the range of our interest $[0 \leq \theta \leq (\pi/2)]$, the coupled pair of integral equations for the potentials

V_1 and V_2 in terms of the linear charge densities may be written down as,

$$V_1 = \frac{1}{4\pi\varepsilon_o}\int_{-\infty}^{\infty} Q'_1(x',\theta)\, K_{11}(x,x')\, dx' + \frac{1}{4\pi\varepsilon_o}\int_{-\infty}^{\infty} Q'_2(\zeta',\theta)\, K_{12}(x,\zeta'\theta)\, d\zeta' \tag{3.6a}$$

$$V_2 = \frac{1}{4\pi\varepsilon_o}\int_{-\infty}^{\infty} Q'_1(x',\theta)\, K_{21}(\zeta,x',\theta)\, dx' + \frac{1}{4\pi\varepsilon_o}\int_{-\infty}^{\infty} Q'_2(\zeta',\theta)\, K_{22}(\zeta,\zeta')\, d\zeta' \tag{3.6b}$$

where the kernels may be written down by inspection as,

$$K_{11}(x,x') = \left[\frac{1}{r_{11}} - \frac{1}{r_{11'}}\right]; \quad K_{12}(x,\zeta',\theta) = \left[\frac{1}{r_{12}} - \frac{1}{r_{12'}}\right] \tag{3.7a}$$

$$K_{21}(\zeta,x',\theta) = \left[\frac{1}{r_{21}} - \frac{1}{r_{21'}}\right]; \quad K_{22}(\zeta,\zeta') = \left[\frac{1}{r_{22}} - \frac{1}{r_{22'}}\right] \tag{3.7b}$$

with

$$r_{11} = [(x-x')^2 + a^2]^{1/2}; \quad r_{11'} = [(x-x')^2 + 4h_1^2]^{1/2} \tag{3.8a}$$

$$r_{12} = [x^2+\zeta'^2-2x\zeta' \cos(\theta) + \alpha^2]^{1/2}$$
$$= [\{\zeta'-x\cos(\theta)\}^2 + \{\alpha^2 + x^2 \sin^2(\theta)\}]^{1/2} \tag{3.8b}$$

$$r_{12'} = [x^2 + \zeta'^2 - 2x\zeta' \cos(\theta) + \beta^2]^{1/2}$$
$$= [\{\zeta'- x\cos(\theta)\}^2 + \{\beta^2 + x^2 \sin^2(\theta)\}]^{1/2} \tag{3.8c}$$

$$r_{21} = [x'^2 + \zeta^2 - 2x'\zeta \cos(\theta) + \alpha^2]^{1/2}$$
$$= [\{x' - \zeta\cos(\theta)\}^2 + \{\alpha^2 + \zeta^2 \sin^2(\theta)\}]^{1/2} \tag{3.8d}$$

$$r_{21'} = [x'^2 + \zeta^2 - 2x'\zeta \cos(\theta) + \beta^2]^{1/2}$$
$$= [\{x' - \zeta\cos(\theta)\}^2 + \{\beta^2 + \zeta^2 \sin^2(\theta)\}]^{1/2} \tag{3.8e}$$

$$r_{22} = [(\zeta-\zeta')^2 + a^2]^{1/2}; \quad r_{22'} = [(\zeta-\zeta')^2 + 4h_2^2]^{1/2} \tag{3.8f}$$

where recall that $\alpha = |h_2 - h_1|$ and $\beta = (h_2 + h_1)$ (3.8g)

Substituting for the total charges $Q'_1(x,\theta)$ and $Q'_2(\zeta,\theta)$ in equation (3.6) from equation (3.1), we have

$$V_1 = \left[Q'_{10} \left\{ \frac{1}{4\pi\varepsilon_o} \int_{-\infty}^{\infty} K_{11}(x,x')\, dx' \right\} + \frac{1}{4\pi\varepsilon_o} \int_{-\infty}^{\infty} q'_1(x',\theta) K_{11}(x,x')\, dx' \right.$$
$$\left. + Q'_{20} \left\{ \frac{1}{4\pi\varepsilon_o} \int_{-\infty}^{\infty} K_{12}(x,\zeta'\theta)\, d\zeta' \right\} + \frac{1}{4\pi\varepsilon_o} \int_{-\infty}^{\infty} q'_2(\zeta',\theta) K_{12}(x,\zeta'\theta)\, d\zeta' \right] \tag{3.6a}$$

$$V_2 = \left[Q'_{10} \left\{ \frac{1}{4\pi\varepsilon_o} \int_{-\infty}^{\infty} K_{21}(\zeta,x',\theta)\, dx \right\} + \frac{1}{4\pi\varepsilon_o} \int_{-\infty}^{\infty} q'_1(x',\theta) K_{21}(\zeta,x',\theta)\, dx' \right.$$
$$\left. + Q'_{20} \left\{ \frac{1}{4\pi\varepsilon_o} \int_{-\infty}^{\infty} K_{22}(\zeta,\zeta')\, d\zeta' \right\} + \frac{1}{4\pi\varepsilon_o} \int_{-\infty}^{\infty} q'_2(\zeta',\theta) K_{22}(\zeta,\zeta')\, d\zeta' \right] \tag{3.6b}$$

The integrals of the kernel functions are somewhat tedious but can be performed to give

$$\left\{ \frac{1}{4\pi\varepsilon_o} \int_{-\infty}^{\infty} K_{11}(x,x')\, dx' \right\} = \frac{1}{2\pi\varepsilon_o} \ell n\left(\frac{2h_1}{a}\right) \equiv S_{11} \tag{3.7a}$$

$$\left\{ \frac{1}{4\pi\varepsilon_o} \int_{-\infty}^{\infty} K_{22}(\zeta,\zeta')\, d\zeta' \right\} = \frac{1}{2\pi\varepsilon_o} \ell n\left(\frac{2h_2}{a}\right) \equiv S_{22} \tag{3.7b}$$

$$\left\{ \frac{1}{4\pi\varepsilon_o} \int_{-\infty}^{\infty} K_{12}(x,\zeta',\theta)\, d\zeta' \right\} = \frac{-1}{4\pi\varepsilon_o} \ell n \left\{ \frac{x^2\sin^2(\theta)+\alpha^2}{x^2\sin^2(\theta)+\beta^2} \right\} \equiv \frac{-f(x,\theta)}{4\pi\varepsilon_o} \tag{3.7c}$$

$$\left\{ \frac{1}{4\pi\varepsilon_o} \int_{-\infty}^{\infty} K_{21}(\zeta,x',\theta)\, dx' \right\} = \frac{-1}{4\pi\varepsilon_o} \ell n \left\{ \frac{\zeta^2\sin^2(\theta)+\alpha^2}{\zeta^2\sin^2(\theta)+\beta^2} \right\} \equiv \frac{-f(\zeta,\theta)}{4\pi\varepsilon_o} \tag{3.7d}$$

Recognizing that $Q'_{10} S_{11} = V_1$ and $Q'_{20} S_{22} = V_2$ for the isolated lines, we arrive at the coupled pair of integral equations for the excess charges given by,

$$\int_{-\infty}^{\infty} q'_1(x',\theta)\, K_{11}(x,x')\, dx' + \int_{-\infty}^{\infty} q'_2(\zeta',\theta)\, K_{12}(x,\zeta',\theta)\, d\zeta' = C'_2 V_2\, f(x,\theta) \tag{3.8a}$$

$$\int_{-\infty}^{\infty} q'_1(x',\theta)\, K_{21}(\zeta,x',\theta)\, dx' + \int_{-\infty}^{\infty} q'_2(\zeta',\theta)\, K_{22}(\zeta,\zeta')\, d\zeta' = C'_1 V_1\, f(\zeta,\theta) \tag{3.8b}$$

In writing above, we have introduced the unperturbed line capacitances of the two transmission lines given by

$$C'_1 = \frac{Q'_{10} - (-Q'_{10})}{V_1 - (-V_1)} = \frac{Q'_{10}}{V_1} = \frac{2\pi\varepsilon_o}{\ell n(2h_1/a)} \equiv \frac{2\pi\varepsilon_o}{\Omega_1} \tag{3.9a}$$

$$C'_2 = \frac{Q'_{20} - (-Q'_{20})}{V_2 - (-V_2)} = \frac{Q'_{20}}{V_2} = \frac{2\pi\varepsilon_o}{\ell n(2h_2/a)} \equiv \frac{2\pi\varepsilon_o}{\Omega_2} \tag{3.9b}$$

and the two forcing functions can be written in a shorthand form as

$$f(\xi,\theta) \simeq \ell n \left\{ \frac{\xi^2 \sin^2(\theta) + \alpha^2}{\xi^2 \sin^2(\theta) + \beta^2} \right\} \tag{3.10}$$

We can now define a capacitive coefficient matrix associated with the excess charges as

$$\begin{bmatrix} q'_1(x,\theta) \\ q'_2(\zeta,\theta) \end{bmatrix} = \begin{bmatrix} k_{11}(x,\theta) & k_{12}(x,\theta) \\ k_{21}(\zeta,\theta) & k_{22}(\zeta,\theta) \end{bmatrix} \begin{bmatrix} V_1 \\ V_2 \end{bmatrix} \tag{3.11}$$

so that

$$k_{11}(x,\theta) = \left.\frac{q'_1(x,\theta)}{V_1}\right|_{V_2 = 0} \tag{3.12a}$$

$$k_{12}(x,\theta) = \left.\frac{q'_1(x,\theta)}{V_2}\right|_{V_1 = 0} \tag{3.12b}$$

$$k_{21}(\zeta,\theta) = \left.\frac{q'_2(\zeta,\theta)}{V_1}\right|_{V_2 = 0} \tag{3.12c}$$

$$k_{22}(\zeta,\theta) = \left.\frac{q'_2(\zeta,\theta)}{V_2}\right|_{V_1 = 0} \tag{3.12d}$$

and the lumped self capacitances in the coupling model are given by,

$$C_1 = \int_{-\infty}^{\infty} [k_{11}(x,\theta) + k_{12}(x,\theta)]\, dx$$

$$= 2 \int_{0}^{\infty} [k_{11}(x,\theta) + k_{12}(x,\theta)]\, dx \tag{3.13a}$$

$$C_2 = \int_{-\infty}^{\infty} [k_{22}(\zeta,\theta) + k_{21}(\zeta,\theta)]\, d\zeta$$

$$= 2 \int_{0}^{\infty} [k_{22}(\zeta,\theta) + k_{21}(\zeta,\theta)]\, d\zeta \tag{3.13b}$$

$$C_m = -\int_{-\infty}^{\infty} k_{12}(x,\theta)\, dx = -2\int_{0}^{\infty} k_{12}(x,\theta)\, dx$$

$$= -\int_{-\infty}^{\infty} k_{21}(\zeta,\theta)\, d\zeta = -2\int_{0}^{\infty} k_{12}(\zeta,\theta)\, d\zeta \qquad (3.13c)$$

We may now set up the integral equations for the excess capacitive coefficients of equation (3.12) by successively considering $V_1 = 0$ and $V_2 = 0$ in equation (3.8).

1. Setting $V_1 = 0$ in equation (3.8) with $V_2 \neq 0$, but finite, leads to

$$\int_{-\infty}^{\infty} k_{12}(x',\theta)\, K_{11}(x,x')\, dx' + \int_{-\infty}^{\infty} k_{22}(\zeta',\theta)\, K_{12}(x,\zeta',\theta)\, d\zeta' = C'_2\, f(x,\theta) \qquad (3.14a)$$

$$\int_{-\infty}^{\infty} k_{12}(x',\theta)\, K_{21}(\zeta,x',\theta)\, dx' + \int_{-\infty}^{\infty} k_{22}(\zeta',\theta)\, K_{22}(\zeta,\zeta')\, d\zeta' = 0 \qquad (3.14b)$$

2. Setting $V_2 = 0$ in equation (3.8) with $V_1 \neq 0$, but finite, leads to

$$\int_{-\infty}^{\infty} k_{11}(x',\theta)\, K_{11}(x,x')\, dx' + \int_{-\infty}^{\infty} k_{21}(\zeta',\theta)\, K_{12}(x,\zeta',\theta)\, d\zeta' = 0 \qquad (3.15a)$$

$$\int_{-\infty}^{\infty} k_{11}(x',\theta)\, K_{21}(\zeta,x',\theta)\, dx' + \int_{-\infty}^{\infty} k_{21}(\zeta',\theta)\, K_{22}(\zeta,\zeta')\, d\zeta' = C'_1\, f(\zeta,\theta) \qquad (3.15b)$$

The remainder of the procedure consists of solving coupled pairs of equations (3.14) and (3.15) for the excess capacitive coefficients and using them in equation (3.13) to get the lumped capacitances.

In concluding this formulation, it is observed that for the special case of $\theta = 0$, using equations (3.3) and (3.7) in (3.6), we obtain

$$V_1 = Q'_{10} S_{11} + q'_{10} S_{11} + Q'_{20} S_{12} + q'_{20} S_{12}$$

$$V_2 = Q'_{10} S_{21} + q'_{10} S_{21} + Q'_{20} S_{22} + q'_{20} S_{22} \qquad (3.16)$$

or, using equation (3.2), (3.16) becomes

$$V_1 = Q_{10} S_{11} + Q_{20} S_{12}$$

$$V_2 = Q_{10} S_{21} + Q_{20} S_{22} \qquad (3.17)$$

with

$$S_{11} = \frac{1}{2\pi\varepsilon_o} \ln\left(\frac{2h_1}{a}\right) ; \quad S_{22} = \frac{1}{2\pi\varepsilon_o} \ln\left(\frac{2h_2}{a}\right) \qquad (3.18)$$

and

$$S_{12} = S_{21} = \frac{1}{2\pi\varepsilon_o} \ln\left(\frac{\beta}{\alpha}\right) = \frac{1}{2\pi\varepsilon_o} \ln\left(\frac{h_2 + h_1}{|h_2 - h_1|}\right)$$

These results for $\theta = 0$, are in complete agreement with the published results in the literature (see for example [1 or 5]).

A. Approximate Analytical Solution

We now develop an approximate analytical solution for the coupled pairs of integral equations (3.14) and (3.15). Rewriting these equations in terms of dimensionless excess capacitive coefficients, we have

$$\int_{-\infty}^{\infty} f_{12}(x',\theta)\, K_{11}(x,x')\, dx' + \int_{-\infty}^{\infty} f_{22}(\zeta',\theta)\, K_{12}(x,\zeta',\theta)\, d\zeta' = f(x,\theta) \tag{3.19a}$$

$$\int_{-\infty}^{\infty} f_{12}(x',\theta)\, K_{21}(\zeta,x',\theta)\, dx' + \int_{-\infty}^{\infty} f_{22}(\zeta',\theta)\, K_{22}(\zeta,\zeta')\, d\zeta' = 0 \tag{3.19b}$$

and

$$\int_{-\infty}^{\infty} f_{11}(x',\theta)\, K_{11}(x,x')\, dx' + \int_{-\infty}^{\infty} f_{21}(\zeta',\theta)\, K_{12}(x,\zeta',\theta)\, d\zeta' = 0 \tag{3.20a}$$

$$\int_{-\infty}^{\infty} f_{11}(x',\theta)\, K_{21}(\zeta,x',\theta)\, dx' + \int_{-\infty}^{\infty} f_{21}(\zeta',\theta)\, K_{22}(\zeta,\zeta')\, d\zeta' = f(\zeta,\theta) \tag{3.20b}$$

where the unknown and normalized excess capacitive coefficients are defined by

$$f_{11}(x',\theta) = k_{11}(x',\theta)\Big/ C_1' \quad ; \quad f_{12}(x',\theta) = k_{12}(x',\theta)\Big/ C_2' \tag{3.21}$$

$$f_{21}(\zeta',\theta) = k_{21}(\zeta',\theta)\Big/ C_1' \quad ; \quad f_{22}(\zeta',\theta) = k_{22}(\zeta',\theta)\Big/ C_2'$$

We now consider solving the coupled integral equation (3.19) and a similar method of solution will apply to equation (3.20) also. To begin with, we expand the excess charges per unit length $q_1'(x',\theta)$ and $q_2'(\zeta',\theta)$ in Taylor series about the points x and ζ respectively. Then, the leading and the first correction terms are given by

$$\begin{aligned} q_1'(x',\theta) &= q_1'(x,\theta) + (x'-x)\,\frac{\partial q_1'}{\partial x}(x,\theta) + \ldots \\ q_2'(\zeta',\theta) &= q_2'(\zeta,\theta) + (\zeta'-\zeta)\,\frac{\partial q_2'}{\partial \zeta}(\zeta,\theta) + \ldots \end{aligned} \tag{3.22}$$

As a result, the unknown functions in equation (3.19) will have expansions given by

$$\begin{aligned} f_{12}(x',\theta) &= f_{12}(x,\theta) + (x'-x)\,\frac{\partial f_{12}}{\partial x}(x,\theta) + \ldots \\ f_{22}(\zeta',\theta) &= f_{22}(\zeta,\theta) + (\zeta'-\zeta)\,\frac{\partial f_{22}}{\partial \zeta}(\zeta,\theta) + \ldots \end{aligned} \tag{3.23}$$

Considering these expansions in the integrals involving the self kernels in equation (3.19), for instance,

$$\begin{aligned} \int_{-\infty}^{\infty} f_{12}(x',\theta)\, K_{11}(x,x')\, dx' &= A_{11} f_{12}(x,\theta) \\ &\quad + \frac{\partial f_{12}}{\partial x}(x,\theta) \int_{-\infty}^{\infty} (x'-x)\, K_{11}(x,x')\, dx' + \ldots \end{aligned} \tag{3.24}$$

where, using equation (3.7a), A_{11} is a constant given by

$$A_{11} = 4\pi\varepsilon_o S_{11} = 2\,\ell n(2h_1/a) \tag{3.25}$$

King [2] has shown that all of the terms in equation (3.24) involving the derivatives of $f_{12}(x,\theta)$ contribute insignificantly compared to the first term under the condition that the radiation from the transmission lines are negligible. As a consequence of this approximation which is well justified at low frequencies, the coupled integral equation (3.19) may be written approximately as

$$A_{11}\, f_{12}(x,\theta) + \int_{-\infty}^{\infty} f_{22}(\zeta',\theta)\, K_{12}(x,\zeta',\theta)\, d\zeta' = f(x,\theta) \qquad (3.26a)$$

$$\int_{-\infty}^{\infty} f_{12}(x',\theta)\, K_{21}(\zeta,x',\theta)\, dx' + A_{22}\, f_{22}(\zeta,\theta) = 0 \qquad (3.26b)$$

where it is recalled that

$$A_{11} = 2\, \ell n(2h_1/a) \quad \text{and} \quad A_{22} = 2\, \ell n(2h_2/a) \qquad (3.27)$$

It is now observed that the above equation can be <u>uncoupled</u> by straightforward algebraic manipulations to obtain,

$$A_{11}\, f_{12}(x,\theta) - \frac{1}{A_{22}} \int_{-\infty}^{\infty} f_{12}(x',\theta)\, T(x,x',\theta)\, dx' = f(x,\theta) \qquad (3.28)$$

$$A_{22}\, f_{22}(\zeta,\theta) - \frac{1}{A_{11}} \int_{-\infty}^{\infty} f_{22}(\zeta',\theta)\, T(\zeta,\zeta',\theta)\, d\zeta' = \frac{1}{A_{11}}\, t(\zeta,\theta) \qquad (3.29)$$

where the various kernels and the forcing functions are given by

$$T(x,x',\theta) = \int_{-\infty}^{\infty} K_{12}(x,\zeta',\theta)\, K_{21}(\zeta',x',\theta)\, d\zeta' \tag{3.30a}$$

$$T(\zeta,\zeta',\theta) = \int_{-\infty}^{\infty} K_{12}(x',\zeta',\theta)\, K_{21}(\zeta,x',\theta)\, dx' \tag{3.30b}$$

$$f(x,\theta) = \ell n \left\{ \frac{x^2 \sin^2(\theta) + \alpha^2}{x^2 \sin^2(\theta) + \beta^2} \right\} \tag{3.30c}$$

$$t(\zeta,\theta) = \int_{-\infty}^{\infty} T(\zeta,\zeta',\theta)\, d\zeta' = - \int_{-\infty}^{\infty} f(x',\theta)\, K_{21}(\zeta,x',\theta)\, dx' \tag{3.30d}$$

similarly,

$$t(x,\theta) = \int_{-\infty}^{\infty} T(x,x',\theta)\, dx' = - \int_{-\infty}^{\infty} f(\zeta',\theta)\, K_{12}(x,\zeta',\theta)\, d\zeta' \tag{3.30e}$$

Once again, using the same approximation as before i.e., essentially retaining the leading terms of the Taylor series expansions of $f_{12}(x',\theta)$ about $f_{12}(x,\theta)$, and of, $f_{22}(\zeta',\theta)$ about $f_{22}(\zeta,\theta)$, in equations (3.28) and (3.29), we have

$$\begin{aligned} A_{11}\, f_{12}(x,\theta) - f_{12}(x,\theta) \left\{ t(x,\theta)/A_{22} \right\} &= f(x,\theta) \\ A_{22}\, f_{22}(\zeta,\theta) - f_{22}(\zeta,\theta) \left\{ t(\zeta,\theta)/A_{11} \right\} &= \left\{ t(\zeta,\theta)/A_{11} \right\} \end{aligned} \tag{3.31}$$

or, the approximate analytical solutions of the coupled pair of integral equation (3.19) are given by

$$f_{12}(x,\theta) \simeq \left[\frac{A_{22}\, f(x,\theta)}{A_{11}A_{22} - t(x,\theta)} \right] \quad ; \quad f_{22}(\zeta,\theta) \simeq \left[\frac{t(\zeta,\theta)}{A_{11}A_{22} - t(\zeta,\theta)} \right] \tag{3.32}$$

This procedure of obtaining an approximate analytical solution can also be applied to the other coupled integral equation (3.20) resulting in similar expressions for $f_{21}(\zeta,\theta)$ and $f_{11}(x,\theta)$. Collecting all the solutions and making use of equation (3.21), we may write the excess capacitive coefficients as

$$k_{11}(x,\theta) = C_1' f_{11}(x,\theta) \simeq C_1' \left[\frac{t(x,\theta)}{A_{11}A_{22} - t(x,\theta)}\right] \tag{3.33a}$$

$$k_{12}(x,\theta) = C_2' f_{12}(x,\theta) \simeq C_2' \left[\frac{A_{22}\, f(x,\theta)}{A_{11}A_{22} - t(x,\theta)}\right] \tag{3.33b}$$

$$k_{21}(\zeta,\theta) = C_1' f_{21}(\zeta,\theta) \simeq C_1' \left[\frac{A_{11}\, f(\zeta,\theta)}{A_{11}A_{22} - t(\zeta,\theta)}\right] \tag{3.33c}$$

$$k_{22}(\zeta,\theta) = C_2' f_{22}(\zeta,\theta) \simeq C_2' \left[\frac{t(\zeta,\theta)}{A_{11}A_{22} - t(\zeta,\theta)}\right] \tag{3.33d}$$

and therefore the normalized capacitances may be calculated using the above in equation (3.13) along with equation (1.1),

$$C_1^{(n1)} = \left(\frac{C_1}{h_1 C_1'}\right) \simeq \int_{-\infty}^{\infty} \left[\frac{t(x,\theta) + A_{11}\, f(x,\theta)}{A_{11}A_{22} - t(x,\theta)}\right] \frac{dx}{h_1} \tag{3.34a}$$

$$C_2^{(n2)} = \left(\frac{C_2}{h_2 C_2'}\right) \simeq \int_{-\infty}^{\infty} \left[\frac{t(\zeta,\theta) + A_{22}\, f(\zeta,\theta)}{A_{11}A_{22} - t(\zeta,\theta)}\right] \frac{d\zeta}{h_2} \tag{3.34b}$$

$$C_m^{(n1)} = \left(\frac{C_m}{h_1 C_1'}\right) \simeq - A_{11} \int_{-\infty}^{\infty} \left[\frac{f(\zeta,\theta)}{A_{11}A_{22} - t(\zeta,\theta)}\right] \frac{dx}{h_1} \tag{3.34c}$$

Equations (3.30) and (3.31) are adequate in evaluating the normalized excess capacitive coefficients (f_{11}, f_{12}, f_{21} and f_{22}) and the normalized lumped capacitive elements of the equivalent circuit in Figure 1.5. In the following subsection, we describe and solve the coupled integral equation (3.16) or (3.17) by an alternate numerical method by casting the integral equations into a system of linear equations. The approximate analytical solution is compared with the numerical solution in Section III-C.

B. Numerical Solution

The set of coupled integral equations (3.19) and (3.20) can also be solved by the method of moments. We may use the symmetry properties summarized below, to economize the calculations.

$$f_{11}(-x,\theta) = f_{11}(x,\theta) \tag{3.35a}$$

$$f_{12}(-x,\theta) = f_{12}(x,\theta) \tag{3.35b}$$

$$f_{21}(-\zeta,\theta) = f_{21}(\zeta,\theta) \tag{3.35c}$$

$$f_{22}(-\zeta,\theta) = f_{22}(\zeta,\theta) \tag{3.35d}$$

The infinite integrals of (3.19) and (3.20) become the following semi-infinite integrals by using the above symmetry relations.

$$\int_0^\infty f_{12}(x',\theta)\, G_{11}(x,x')\, dx' + \int_0^\infty f_{22}(\zeta',\theta)\, G_{12}(x,\zeta',\theta)\, d\zeta' = f(x,\theta) \tag{3.36a}$$

$$\int_0^\infty f_{12}(x',\theta)\, G_{21}(\zeta,x',\theta)\, dx' + \int_0^\infty f_{22}(\zeta',\theta)\, G_{22}(\zeta,\zeta')\, d\zeta' = 0 \tag{3.36b}$$

and

$$\int_0^\infty f_{11}(x',\theta)\, G_{11}(x,x')\, dx' + \int_0^\infty f_{21}(\zeta',\theta)\, G_{12}(x,\zeta',\theta)\, d\zeta' = 0 \tag{3.37a}$$

$$\int_0^\infty f_{11}(x',\theta)\, G_{21}(\zeta,x',\theta)\, dx' + \int_0^\infty f_{21}(\zeta'\theta)\, G_{22}(\zeta,\zeta')\, d\zeta' = f(\zeta,\theta) \tag{3.37b}$$

where the new kernels are

$$G_{11}(x,x') = K_{11}(x,x') + K_{11}(x,x') \tag{3.38a}$$

$$G_{12}(x,\zeta',\theta) = K_{12}(x,\zeta',\theta) + K_{12}(x,-\zeta',\theta) \tag{3.38b}$$

$$G_{21}(\zeta,x',\theta) = K_{21}(\zeta,x',\theta) + K_{21}(\zeta,-x',\theta) \tag{3.38c}$$

$$G_{22}(\zeta,\zeta') = K_{22}(\zeta,\zeta') + K_{22}(\zeta,-\zeta') \tag{3.38d}$$

In order to use the moment method, we divide x into x_i, $i = 0,1,2, \ldots, N$; and ζ into ζ_i, $i = 0,1,2, \ldots, N$. The values x_i are taken to be equal to ζ_i for convenience. The points x_N and ζ_N are the truncation points for the moment method. It is expected that the charge density near the junction region of the wires changes fairly rapidly, and decays slowly to zero when x or ζ is very large. Hence the two different mesh sizes are considered: from x_0 to x_{N_1} the smaller meshes are used, and from x_{N_1} to x_N, we may use large meshes. The breaking point x_{N_1} was found to be very closely related to the right-hand-side vector $f(x,\theta)$.

For brevity, we shall consider equation (3.36). Let us assume

$$q_{12}^i = f_{12}(x_i,\theta) \quad \text{and} \quad q_{22}^i = f_{22}(\zeta_i,\theta) \tag{3.39}$$

Using the linear basis functions, we find that (3.36) can be evaluated by

$$\sum_{i=0}^{N} q_{12}^i \, I_{11}^{i,j} + \sum_{i=0}^{N} q_{22}^i \, I_{12}^{i,j} = f(x_j,\theta) \tag{3.40a}$$

$$\sum_{i=0}^{N} q_{12}^{i} I_{21}^{i,j} + \sum_{i=0}^{N} q_{22}^{i} I_{22}^{i,j} = 0 \qquad (3.40b)$$

where

$$I_{uv}^{i,j} = \delta_{i0} \int_{x_{i-1}}^{x_i} \frac{x' - x_{i-1}}{x_i - x_{i-1}} G_{uv}(x_j, x')\, dx'$$

$$+ \delta_{iN} \int_{x_i}^{x_{i+1}} \frac{x' - x_{i+1}}{x_i - x_{i+1}} G_{uv}(x_j, x')\, dx' \; ; \quad u = 1,2; \; v = 1,2 \qquad (3.41)$$

$$\delta_{ik} = \begin{cases} 1 & \text{if } i = k \\ 0 & \text{if } i \neq k \; . \end{cases}$$

Since $x_i = \zeta_i$, the variables x and ζ are interchangable in equation (3.41). The integrations of (3.41) can be evaluated analytically. By reviewing equation (3.38), (3.7), and (3.8), we find that all the integrations in (3.41) are of the following type:

$$\int_{u_1}^{u_2} \frac{r_3 x' + r_4}{[(x' - r_1)^2 + r_2]^{1/2}}\, dx' = r_3 \left[\sqrt{u_2^2 - 2r_1 u_2 + r_1^2 + r_2} - \sqrt{u_1^2 - 2r_1 u_1 + r_1^2 + r_2} \right]$$

$$+ (r_4 + r_3 r_1) \left[\operatorname{arcsinh}\left(\frac{u_2 - r_1}{\sqrt{r_2}} \right) - \operatorname{arcsinh}\left(\frac{u_1 - r_1}{\sqrt{r_2}} \right) \right] \qquad (3.42)$$

A total number of (2N + 2) linear equations can be formulated from equation (3.40) by taking $j = 0,1,2, \ldots, N$. The (2N + 2) unknowns, q_{12}^{i} and q_{22}^{i} can then be readily solved by matrix methods. The values of $f_{21}(x_i,\theta)$ and $f_{22}(\zeta_i,\theta)$ can also be solved in a similar manner.

The lumped capacitances can be obtained from equations (1.1), (3.13), and (3.18). They are

$$c_1^{(n1)} = \frac{1}{h_1}\int_{-\infty}^{\infty}\left[f_{11}(x,\theta) + f_{12}(x,\theta)\right] dx$$

$$= \frac{2}{h_1}\int_{0}^{\infty}\left[f_{11}(x,\theta) + f_{12}(x,\theta)\right] dx \qquad (3.43a)$$

$$c_2^{(n2)} = \frac{1}{h_2}\int_{-\infty}^{\infty}\left[f_{22}(\zeta,\theta) + f_{21}(\zeta,\theta)\right] d\zeta$$

$$= \frac{2}{h_2}\int_{0}^{\infty}\left[f_{22}(\zeta,\theta) + f_{22}(\zeta,\theta)\right] d\zeta \qquad (3.43b)$$

$$c_m^{(n1)} = -\frac{1}{h_1}\int_{-\infty}^{\infty} f_{21}(\zeta,\theta)\, d\zeta$$

$$= -\frac{2}{h_1}\int_{-\infty}^{\infty} f_{21}(\zeta,\theta)\, d\zeta \qquad (3.43c)$$

This completes a brief description of the numerical method of solving the coupled integral equations. In the following subsection, we compare the approximate analytical solution with the numerical solution and present the capacitance data as well.

C. Discussion of Results

In this section we present the results of a parametric study of the normalized excess charges and the normalized lumped capacitances in the equivalent circuit of Figure 1.5. It is recalled that, to obtain the normalized excess charges, one has to solve a set of coupled integral equations (3.19) and (3.20). Owing to a lack of experimental data on this problem, and also to ensure confidence in the solution, the coupled integral equations have been solved by two different methods. In Section III-A, an approximate analytical solution which leads to a closed integral form for the excess charges was presented. On the other hand, Section III-B described a numerical method of solving the same set of coupled integral equations.

In Figures 3.1 to 3.4, we compare the normalized excess charge distributions along the transmission lines, obtained by the two methods. This comparison is done graphically for the four representative cases;

a) $(h_2/h_1) = 1.5$, $\theta = 15°$ b) $(h_2/h_1) = 1.5$, $\theta = 90°$

c) $(h_2/h_1) = 5$, $\theta = 15°$ d) $(h_2/h_1) = 5$, $\theta = 90°$

The normalized excess charges are plotted as a function of normalized coordinates (x/h_1) and (ζ/h_1), starting from the junction region and moving along the transmission lines. It is seen from the Figures 3.1 to 3.4, that for all the four cases, the agreement between the approximate

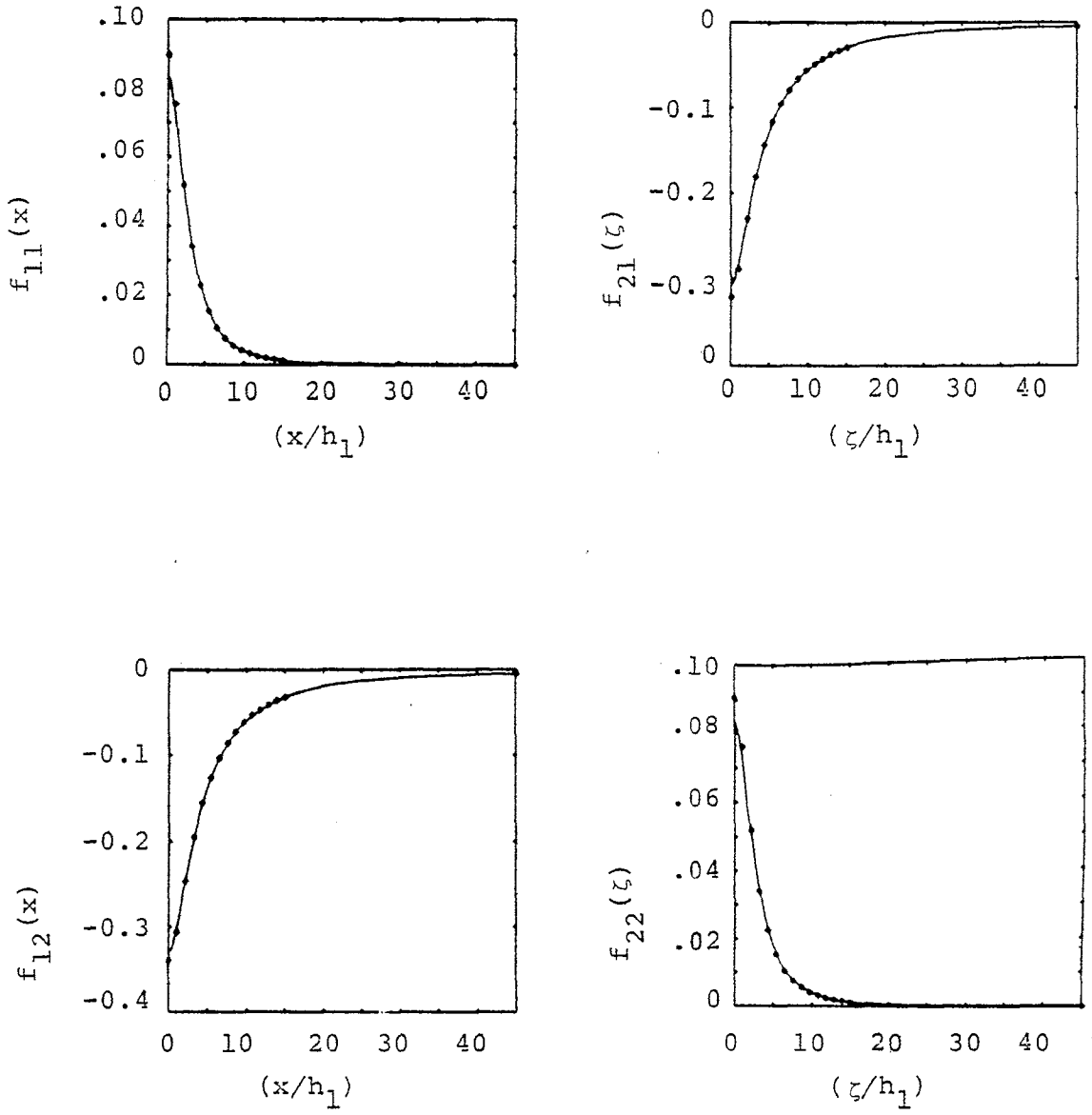

Figure 3.1. Normalized excess charge distributions along the two transmission lines; $(h_2/h_1) = 1.5$, $(a/h_1) = 0.01$, $\theta = 15°$; _____ approximate analytical solution, ... numerical solution

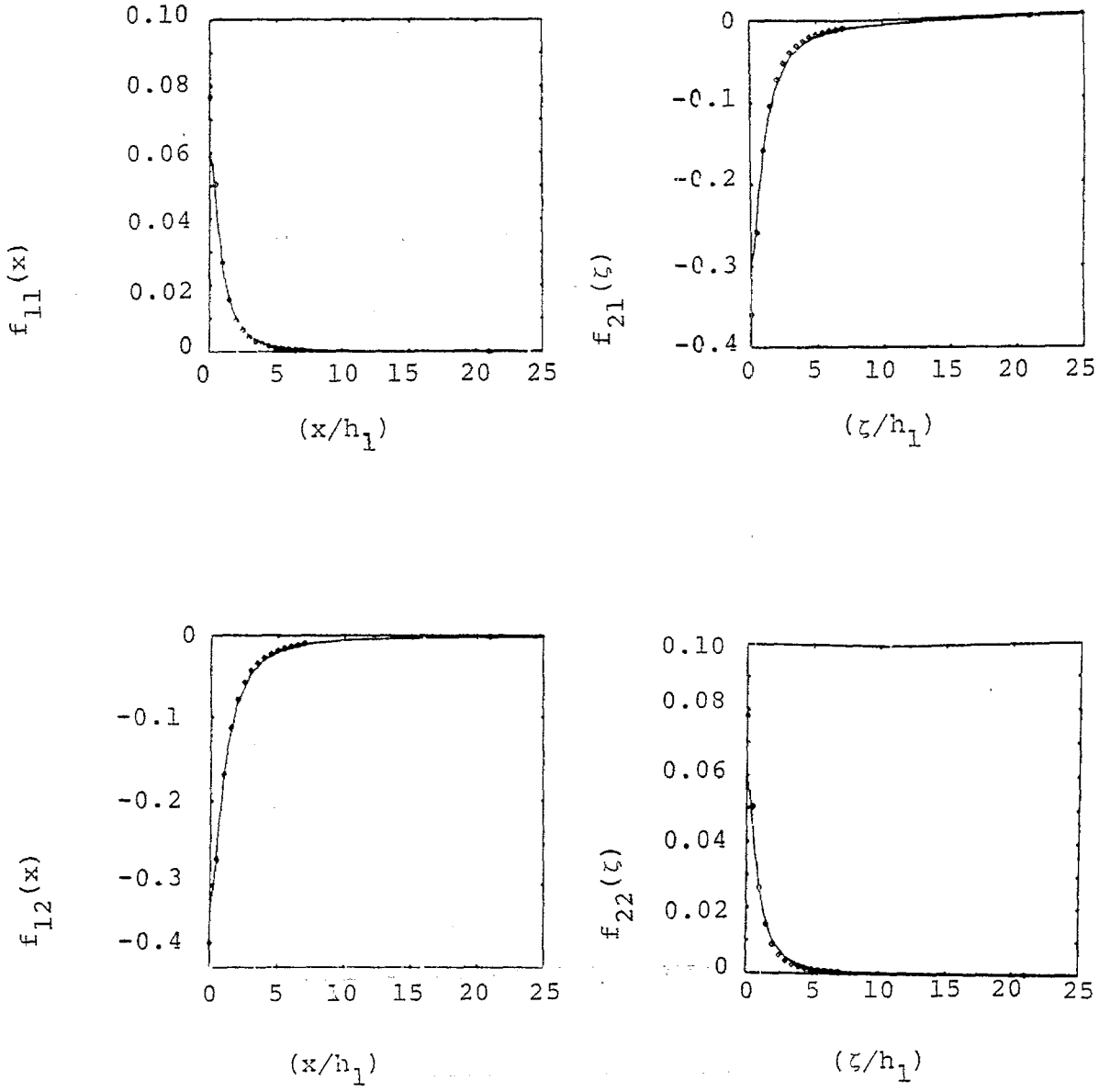

Figure 3.2. Normalized excess charge distributions along the two transmission lines; $(h_2/h_1) = 1.5$, $(a/h_1) = 0.01$, $\theta = 90°$; _____ approximate analytical solution, ... numerical solution

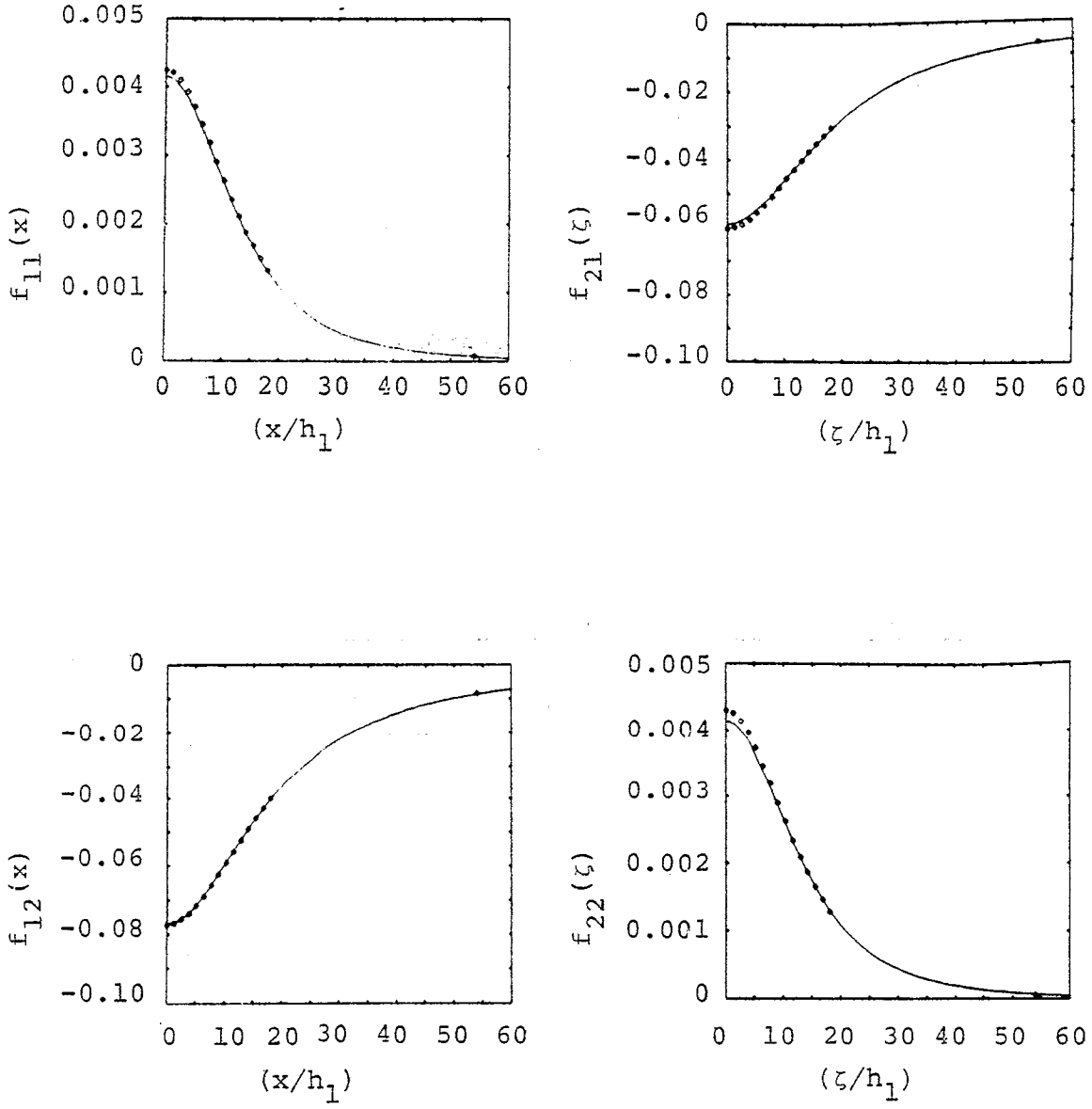

Figure 3.3. Normalized excess charge distributions along the two transmission lines; $(h_2/h_1) = 5.0$, $(a/h_1) = 0.01$, $\theta = 15°$ _____ approximate analytical solution, ... numerical solution

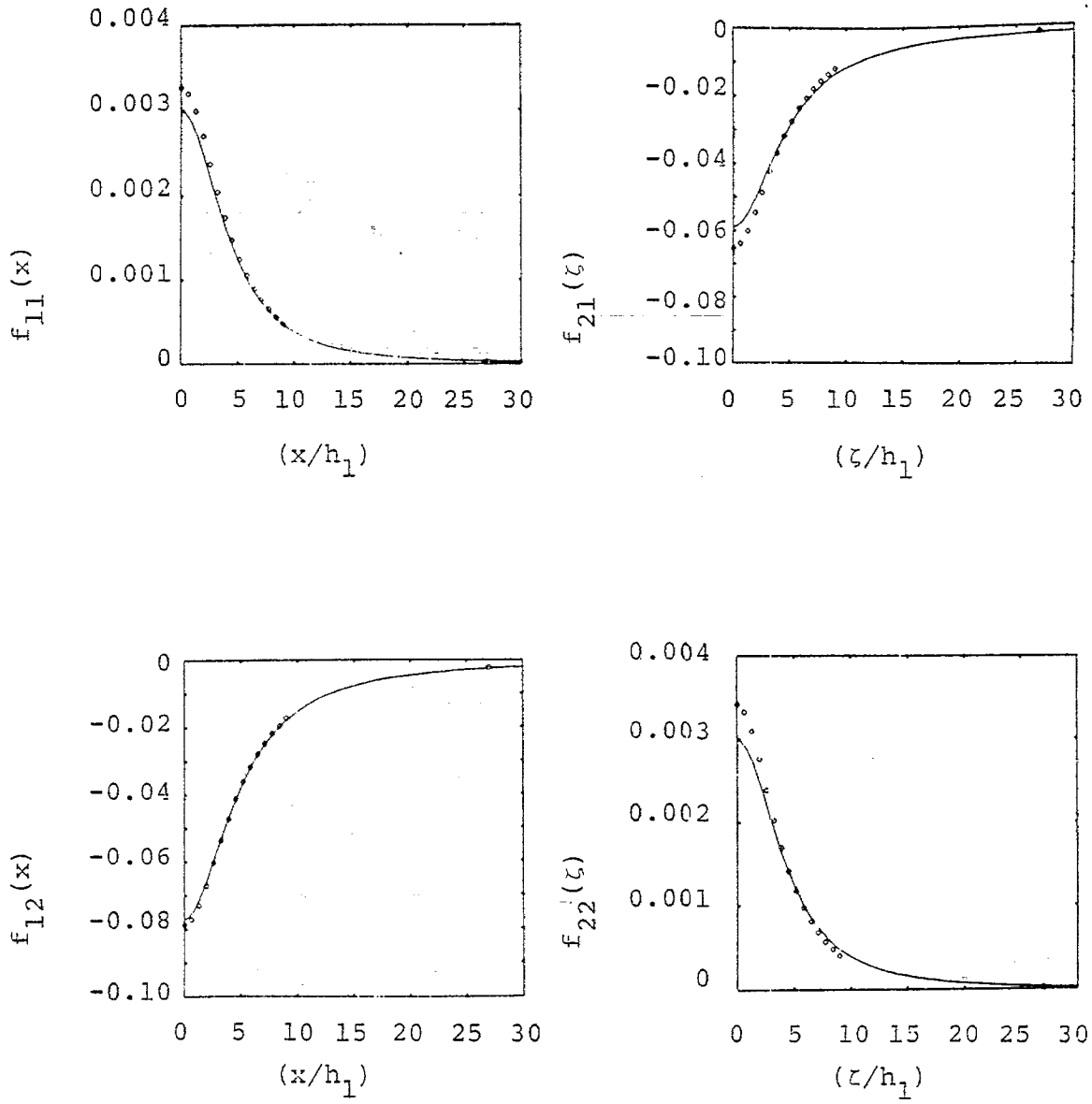

Figure 3.4. Normalized excess charge distributions along the two transmissions; $(h_2/h_1) = 5.0$, $(a/h_1) = 0.01$, $\theta = 90°$; _____ approximate analytical solution, ... numerical solution

analytical and the numerical solution is excellent. Furthermore, as may be expected, the normalized excess charges have a peak at the junction and decay as one moves away from the junction.

The normalized excess charges computed from the approximate analytical solution can then be used in computing the normalized lumped capacitive elements via equation (3.34) or (3.43). The capacitance plots are parametrically displayed in Figures 3.5 and 3.6.

In Figure 3.5, the normalized lumped capacitances are plotted as a function of the skew angle which ranges from small angles to 90°. The case of $\theta = 0°$ is excluded here, because of the distributed interaction and has been considered elsewhere in this report. As expected, Figure 3.5 shows that as the height of the top line is increased, the self capacitance terms decrease.

Figure 3.6, graphically shows the normalized lumped capacitances as a function of the relative height (h_2/h_1) with the skew angle θ as a parameter. Once again, we see the expected behavior as the skew angle or the relative height is varied.

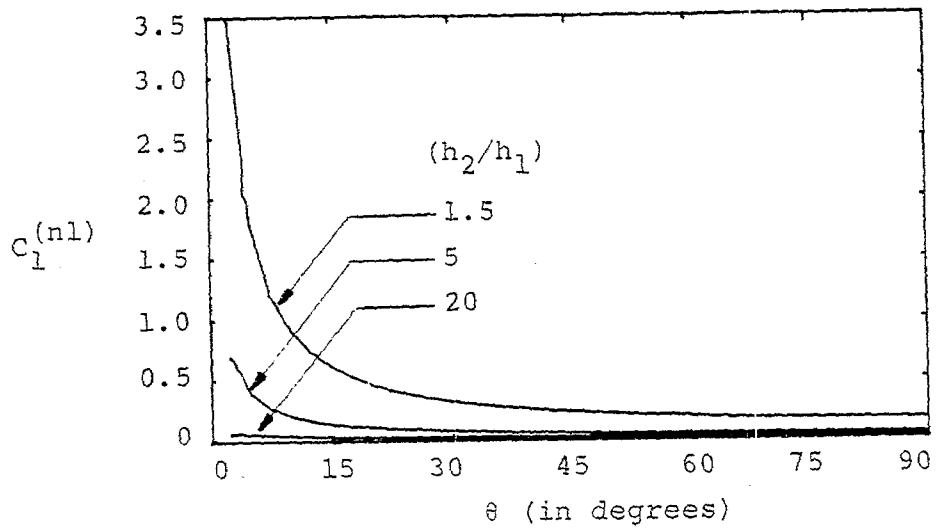

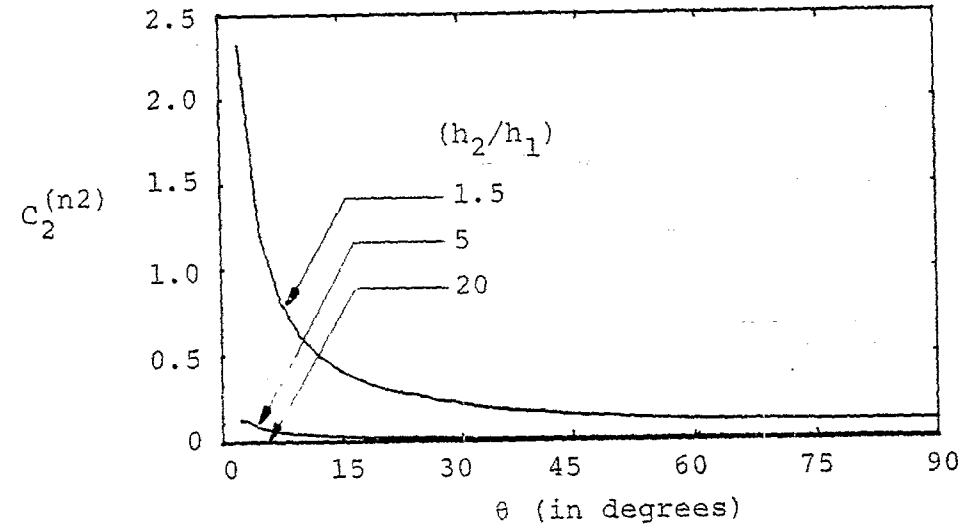

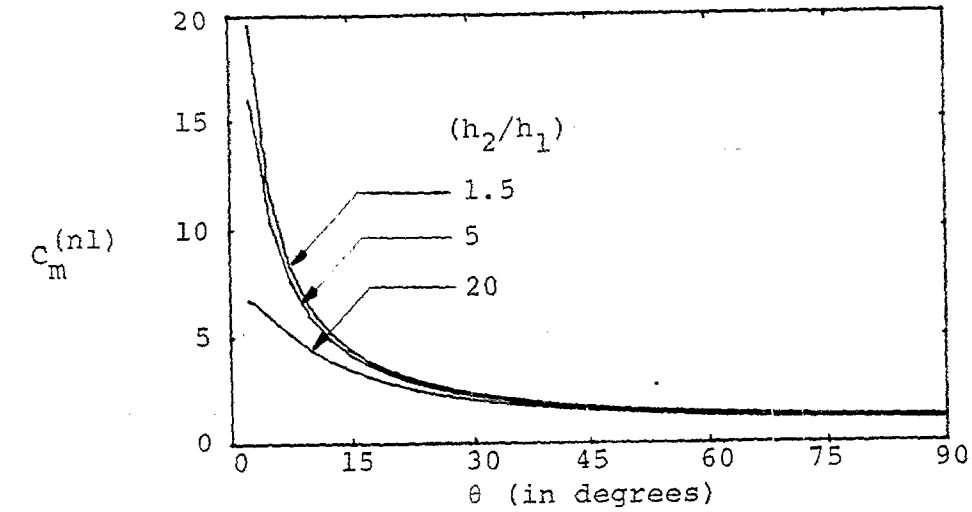

Figure 3.5 Normalized lumped capacitances as a function of skew angle.

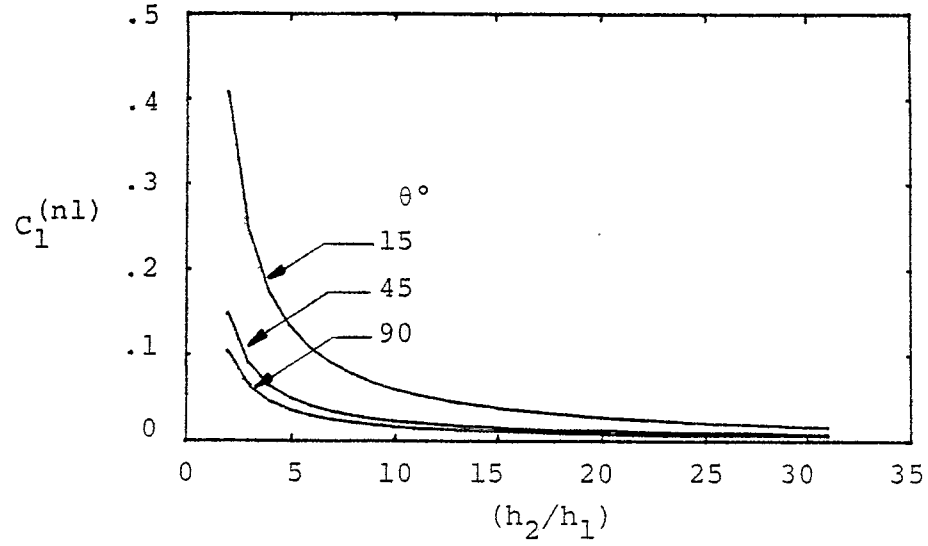

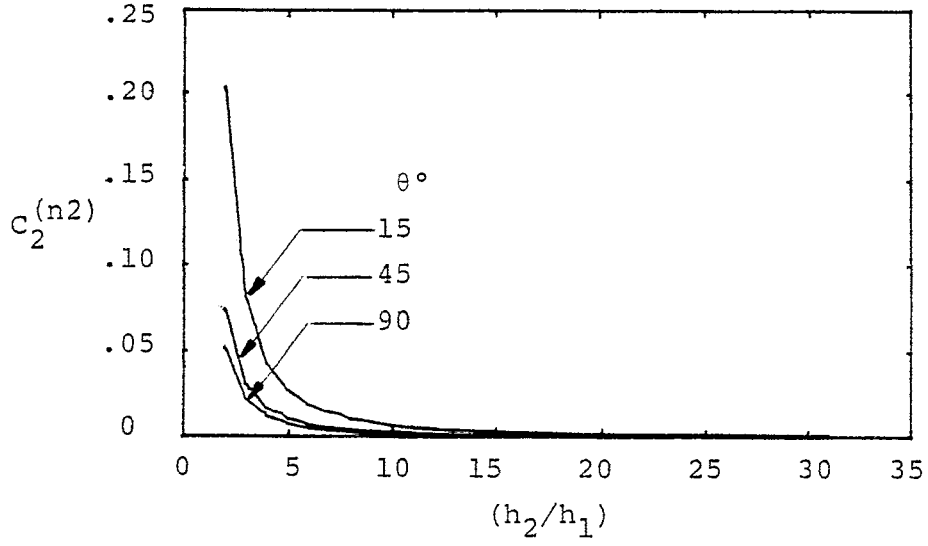

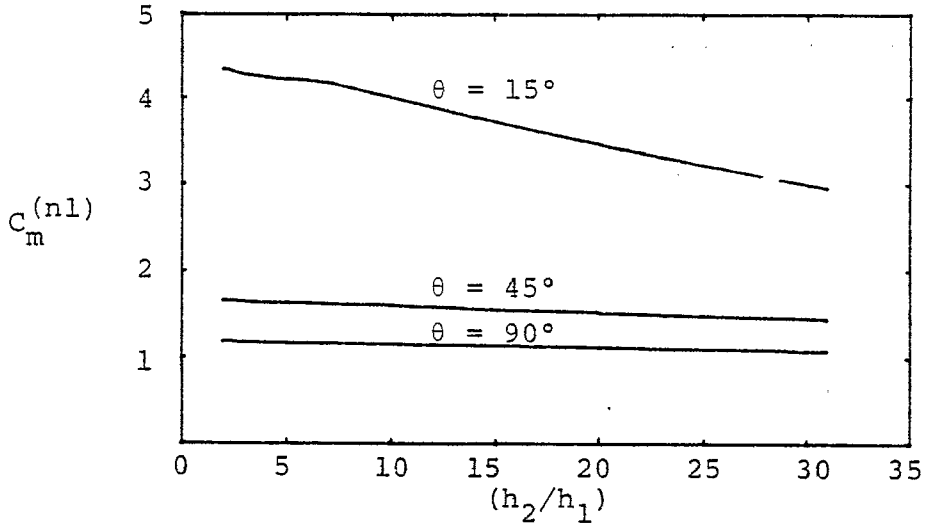

Figure 3.6 Normalized lumped capacitances as a function of relative height.

IV. Conclusions

In this report, the problem of obtaining the lumped equivalent circuit to represent the junction region of a pair of skewed transmission lines is presented. The coupling model involves evaluating the inductive and capacitive elements. The mutual inductance is evaluated in a closed form and has been parametrically displayed. To obtain the capacitive elements, a set of coupled integral equations have been formulated for the excess charge distributions. The integral equations have been solved by an approximate analytical method and also a numerical method employing the method of moments. The approximate analytical solution uses a Taylor series expansion of the unknown functions about a variable, and enables one to express the excess charges in closed form using a single integration. The two independent calculations of the normalized excess charge distributions are compared graphically for representative cases and seen to be in excellent agreement. Once the excess charge distributions are determined, it is a simple matter to evaluate the normalized lumped capacitances. The results of a parametric study of the capacitance computations are also presented.

APPENDIX A

Transmission Line Coupling for the Special Case of $\theta = 0$

In this appendix, we consider the special case of distributed interaction between the two transmission lines (see Figure 1.1) when the skew angle θ is zero. In other words, the two wires are parallel to each other and are located at heights h_1 and h_2 above a perfectly conducting ground plane. In this case, one cannot derive a junction equivalent circuit because of the distributed interaction between the wires. Using the same notation as in Section III, the total charges per unit length Q'_{10} and Q'_{20} may be related to the potentials V_1 and V_2 on the two wires with respect to the ground plane, via the capacitance per unit length matrix [C'] given by

$$\begin{bmatrix} Q'_{10} \\ Q'_{20} \end{bmatrix} = \begin{bmatrix} C'_{11} & C'_{12} \\ C'_{21} & C'_{22} \end{bmatrix} \begin{bmatrix} V_1 \\ V_2 \end{bmatrix} \tag{A.1}$$

It was seen in Section III that the elements of the coefficients of elastance matrix [S'] are given by

$$\left[S'_{n,m}\right] = \left[C'_{n,m}\right]^{-1} \tag{A.2}$$

$$S'_{11} = \frac{1}{2\pi\varepsilon_o} \ln\left(\frac{2h_1}{a}\right) \; ; \quad S'_{22} = \frac{1}{2\pi\varepsilon_o} \ln\left(\frac{2h_2}{a}\right) \tag{A.3}$$

$$S'_{12} = S'_{21} = \frac{1}{2\pi\varepsilon_o} \ln\left(\frac{\beta}{\alpha}\right) = \frac{1}{2\pi\varepsilon_o} \ln\left(\frac{h_2 + h_1}{|h_2 - h_1|}\right) \tag{A.4}$$

These results are in complete agreement with the results reported in the literature [1]. The elements of the [C] matrix are then given by

$$C'_{11} = (S'_{22}/\Delta) \; ; \quad C'_{22} = (S'_{11}/\Delta) \tag{A.5}$$

$$C'_{12} = C'_{21} = (-S'_{12}/\Delta) \tag{A.6}$$

where

$\Delta \equiv$ determinant of the S matrix

$$= \left(\frac{1}{2\pi\varepsilon_o}\right)^2 \left[\ell n\left(\frac{2h_1}{a}\right)\ell n\left(\frac{2h_2}{a}\right) - \ell n\left(\frac{\beta}{\alpha}\right)\ell n\left(\frac{\beta}{\alpha}\right)\right] \tag{A.7}$$

Furthermore, the inductance per unit length matrix is simply related to the [S'] matrix as

$$\left[L'_{n,m}\right] = \mu_o\varepsilon_o\left[S'_{n,m}\right] \tag{A.8}$$

so that,

$$L'_{11} = \left(\frac{\mu_o}{2\pi}\right)\ell n\left(\frac{2h_1}{a}\right) \; ; \quad L'_{22} = \left(\frac{\mu_o}{2\pi}\right)\ell n\left(\frac{2h_2}{a}\right) \tag{A.9}$$

$$L'_{12} = L'_{21} = \left(\frac{\mu_o}{2\pi}\right)\ell n\left(\frac{\beta}{\alpha}\right) \tag{A.10}$$

We have included this special case of $\theta = 0$ in this appendix mainly in the interest of completeness. These results are available in the literature and serve to check the consistency of our formulation in a limiting situation.